A NEW FINITE ELEMENT METHOD FOR ANALYSIS OF H-PLANE WAVEGUIDE JUNCTIONS

by

Andy M. Froncioni, B. Eng., B.Sc.

A thesis submitted to the Faculty of Graduate Studies and Research in partial fulfillment of the requirements for the degree of Master of Engineering

Department of Electrical Engineering
McGill University
Montréal, Canada
April, 1988

To my parents,

Acknowledgements

Many people have contributed to the preparation of this document, to which I am endebted. I would like to express my deepest thanks to my supervisor, Dr. Jon Webb, for his guidance, support, and understanding throughout my Master's studies. His thoroughness and honesty are an inspiration to myself and others in the CADLAB.

I am also greatly endebted to Toufic Boubez, whose friendship and understanding were limitless. Without his help I would surely not have finished. I won't forget the help he gave me...

I would also like to thank Kalli Varaklis for her unwavering support and patience during last few months of this degree. Thanks, Kal.

I would like to also thank Matt Cendamo for his support and for the preparation of the figures. Also, Pablo Garcia for the way he was always willing to help, in any way possible and to Jennifer Ralston for her help and words of encouragement.

Special thanks are in order for Bill Kanellopoulos and Chris Crowley for their technical advice in electromagnetics and their constant willingness to help, Amy Pinchuk and Steve McFee for their great lab spirit, and the rest of the CADLAB for putting a little fun into research.

In addition, I would like to express my gratitude to Dr. John Addison of the McGill Physics Department, who taught me introductory electromagnetics in a way that I could never forget it. He is certainly one of the finest teachers that I have ever had.

Last, but certainly not least, I would like to thank my parents for their understanding and support through even the hardest times, and for always having had faith in me...and Mike, who is as much a friend as a brother.

Abstract

The determination of network parameters for arbitrarily-shaped waveguide junctions is best handled by numerical methods. Recently, several methods have emerged for obtaining these parameters for H-plane waveguide junctions [1] [2] [3] [4] using the finite element method. These methods, however, all have restrictions regarding the placement of the planes which define the location of the ports of the junction. This thesis presents a finite element method to extract network parameters of H-plane waveguide junctions, which is free of the previous methods' restrictions. The new method makes use of modal projection operators which account for evanescent modes at the ports. The new formulation generates a matrix equation which, under certain conditions, is positive definite, leading to faster solution times. Results from a FORTRAN implementation for several test examples are presented.

Résumé

Les procédés numériques s'attaquent bien à la détermination des coéfficients d'impédance pour les jonctions de géométries générales. Récement, plusieurs procédés qui utilisent la théorie des éléments finis ont étés présentés pour les jonctions dans le plan H [1] [2] [3] [4]. Cependant, ces procédés ont tous des réstrictions sur le placement des plans de portails. Cette thèse présente un procédé d'élément finis qui extrait les coéfficients d'impédance d'une jonction de plan H sans ces réstrictions. Ce nouveau procédé utilise des opérateurs modals qui calculent les champs électriques dûs aux modes décroissants dans les guides d'ondes. Le nouveau procédé produit une équation de matrice qui est définie positive dans certains cas. On peut donc résoudre ce système plus vite. Les résultats obtenus d'un logiciel écrit en FORTRAN pour plusieurs problèmes de jonction concordent bien avec la théorie.

TABLE OF CONTENTS

Chapter 1 - Introduction

Waveguides are structures which are used to transmit high-frequency signals from one device to another. The region at which several waveguides meet is called a waveguide junction. Phase-shifters, attenuators, and matched terminations are examples of waveguide junctions. Figure 1.1 depicts several more.

It is often useful to characterise these junctions as N-port devices with NxN scattering matrices relating the energy-coupling between the dominant mode waves at the ports. This allows a given junction to be represented as a network element. However, the derivation of the network parameters for an arbitrary waveguide junction requires either measurement or the solution of electromagnetic field problems, that is, the solution of the fields which result from the application of Maxwell's equations.

Experimental methods for solving electromagnetic problems are often expensive and time-consuming. Theoretical solution techniques may be either analytic or numerical. Analytic methods are usually geometry- or problem-dependent and hence lack the flexibility required in a computational tool for waveguide analysis. It is therefore sometimes desirable to use numerical methods to solve electromagnetic boundary value problems. Methods such as finite elements have the advantage that they may be formulated so as to be geometry-independent.

The fundamental equation to solve in waveguide analysis is the curl-curl

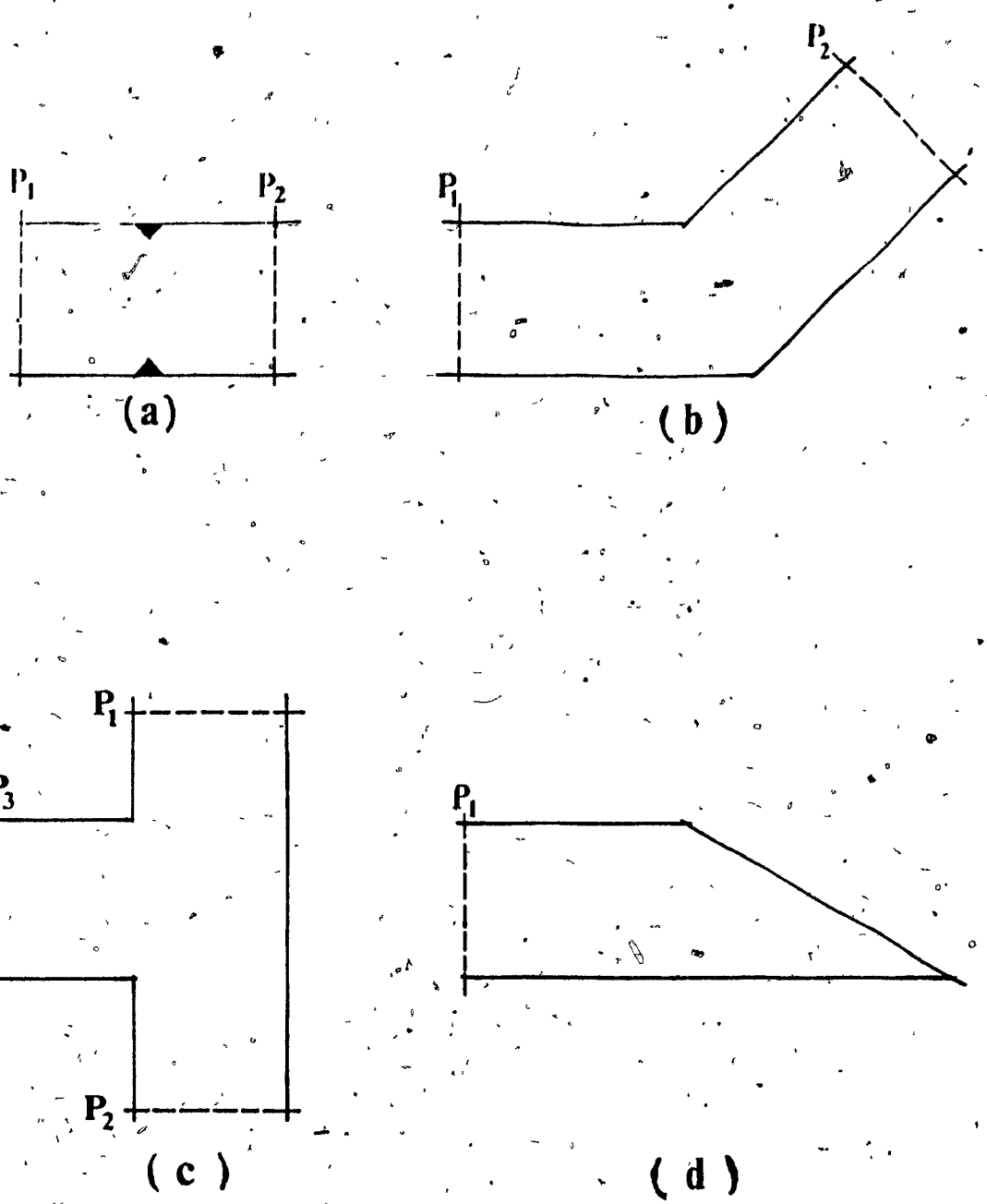

FIG 1.1 SOME WAVEGUIDE JUNCTIONS

(a) Capacitive obstacle
(b) Waveguide Bend
(c) T-Junction
(d) Waveguide Termination

equation, a variation of the vector Helmholtz equation. The general problem of solving for the fields in a junction is intrinsically three-dimensional in nature. However, a two-dimensional analysis may be appropriate if the variation in the fields are known in a given direction. An example of this is an H-plane electric field problem in which the junction geometry is constant in the y-direction (Figure 1.2). In such a problem, only the y-component of electric field exists. Therefore, a one-component, two-dimensional analysis is valid.

Recently, several finite element methods ([1][2][3][4]) have been proposed to extract the network parameters of arbitrarily-shaped, H-plane waveguide junctions. All of these methods impose some limitation on the placement of the port planes that define the extent of the junction. In Webb[1] the port planes must be sufficiently far from the junction cavity so that the transverse fields at the port planes are effectively composed of only the dominant mode. In Koshiba et. al. [2][3][4], two port planes must be defined, for each waveguide connected to the junction, in order to account for the field contributions of evanescent modes at the port planes. It is necessary to mesh the problem so that there are a significant number of nodes between the planes in each waveguide. In both methods, there is a degree of uncertainty about the position of the port planes. This represents an inconvenience to the user of this type of formulation.

The aim of this thesis is to present a finite element formulation to extract network parameters of an arbitrarily-shaped H-plane waveguide junction which is free of the port plane restrictions found in Webb[1] and Koshiba et. al [2][3][4]. The new method presented allows the user to define the extent of the junction region with as little knowledge as possible of the fields within the device. In addition, the new formulation is cast in terms of a positive definite matrix operator in some cases, thereby enabling faster solution times.

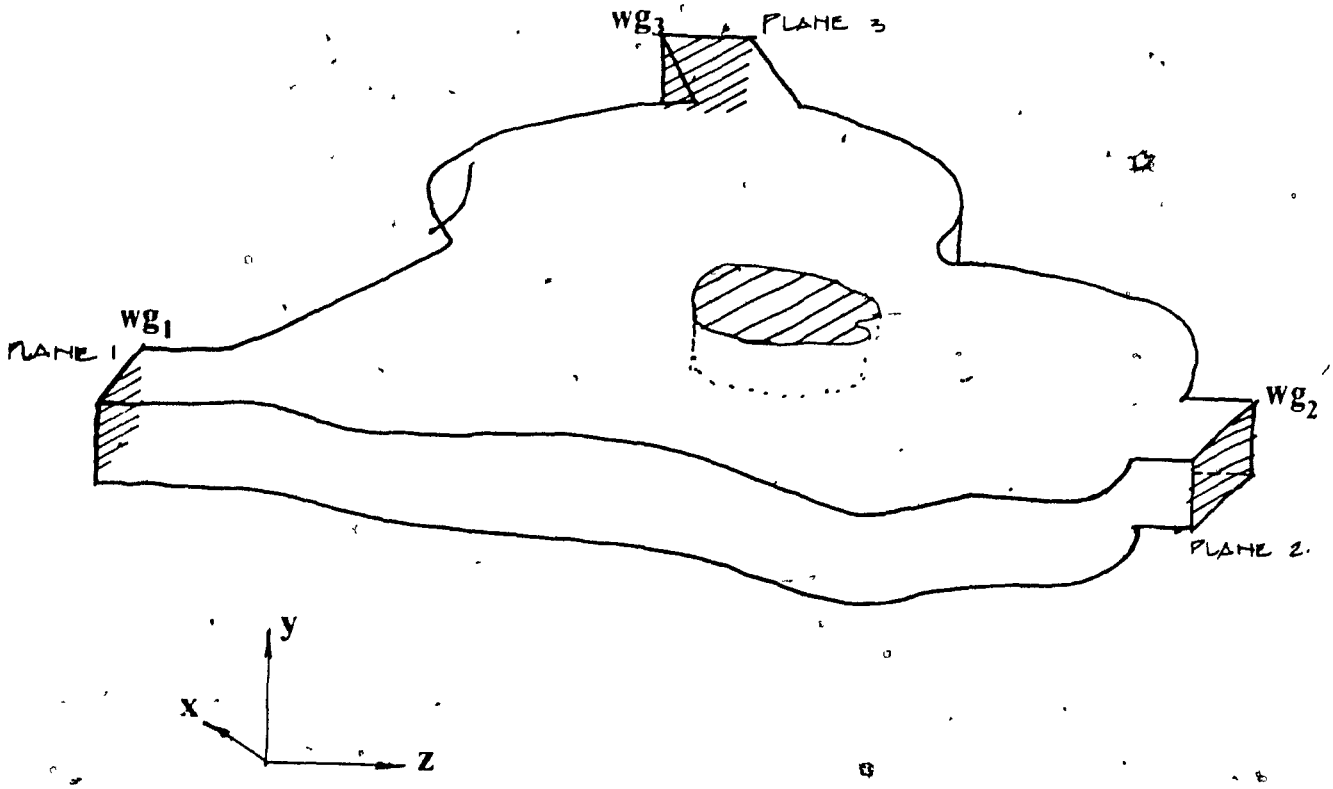

FIG 1.2 AN H-PLANE WAVEGUIDE JUNCTION

The thesis is organised as follows: Chapter 2 provides a history of past work in computational waveguide analysis. Chapter 3 presents some relevant electromagnetic theory. The finite element analysis of waveguide junctions is discussed in Chapter 4. In Chapter 5, a new finite element formulation is presented and Chapter 6 deals with the implementation of the method and results obtained from some test examples. A discussion of the merits and disadvantages of the new method is given in Chapter 7, which serves as a Conclusion. The Appendices provide relevant proofs and some background functional analysis.

Chapter 2 - Literature Survey

This Chapter will present an overview of past work in waveguide analysis, with emphasis on numerical methods.

Early waveguide analysis relied primarily upon experimental, analytical, semi-analytical and graphical techniques [5][6][7] . In the mid-forties, Southwell [8] applied relaxation techniques to a number of physical problems involving the solution to Laplace's equation. This analysis led to another paper by Grad [9] which investigated the utility of this type of analysis in dealing with a number of electrical engineering problems, including *TEM*-mode waveguide analysis. In addition, Grad extended Southwell's relaxation approach to develop a method to determine the resonant modes of a waveguide cavity.

In the early sixties, Davies [10][11] proposed a semi-analytic method which was applied to an N-port H-plane junction to determine its scattering parameters. This analysis, however, ignored contributions to the field at the port planes due to evanescent modes and, consequently, the port planes needed to be placed sufficiently far from the junction cavity so that only the dominant- mode fields are significant. By the mid-sixties, finite difference schemes for transmission-line and waveguide analysis were developed by Green [12], Schneider [13], and Metcalfe [14]

for TEM-mode analysis. The principal shortcoming of these methods was, due to the regular grids necessary in the finite difference method, that curved-boundary problems could not be analysed. This restriction was removed by Carson [15] in a formulation in which the boundary nodes of the problem region were treated using a special difference scheme.

Later, an E- and H-plane finite difference formulation was introduced by Muilwyk and Davies [16]. In their paper, the authors acknowledged the limitations of an analysis that neglects the presence of evanescent waveguide modes at the port planes, in determining network parameters, as in Davies[10][11]. This port plane restriction was partially eliminated in the mode-matching method of Wexler [17]. Here, reflection and transmission coefficients of systems of connected waveguides were obtained by ensuring continuity of a finite number of waveguide modes. However, the analysis required a great deal of computational effort and was ineffective in treating arbitrary-shaped structures.

Finite element formulations to analyse waveguide components emerged in the late sixties. Ahmed [18] proposed an axial field (E_z, H_z) method from which the other components of electric and magnetic field could be extracted. The method determined the propagating modes and resonant frequencies of arbitrarily-shaped, dielectric-filled waveguide structures. Later, Silvester [19] outlined a finite element method to determine the modes and resonant frequencies of two-dimensional, scalar Helmholtz field problems. In a subsequent paper, Silvester [20] used an H-plane, scalar formulation to determine the admittance parameters of an N-port stripline or microstrip junction. However, the restrictions mentioned in Muilwyk and Davies [16] remained, namely; port planes needed to be placed a large distance from the junction cavity.

By the mid-seventies, two- and three-dimentional finite element formulations had been developed by Konrad [21][22] and Ferrari et. al.[23] to solve for fields in waveguide components. These methods were extended by Webb [1][24] to obtain impedance and admittance parameters of H-plane junctions, subject to the port plane restriction. Recently, however, Koshiba et.al. [2][3][4][25] have developed waveguide junction formulations (E-plane and H-plane) which account for evanescent modes at the port planes, thereby removing this restriction. However, their method requires the modeling of two planes per port with a significant number of nodes in the region between the two planes. In addition, the matrix equation arising from this formulation is not symmetric, thus increasing solution time. The development of a less restrictive formulation, such as the one presented in this thesis, is therefore motivated.

Chapter 3 - Some Waveguide Theory

This chapter will deal with some electromagnetic theory needed to describe waveguide junctions. The Chapter will begin with a presentation of the waveguide field problem and the corresponding mathematical formulation. Next, the waveguide junction will be introduced as will its equivalent circuit parameters and a method to determine these parameters. Finally, the H-plane rectangular waveguide problem will be presented and discussed. For simplicity, the theory will deal with single-mode waveguide operation only.

3.1 - The Waveguide

A waveguide is a structure through which a high-frequency electromagnetic signal may be sent (see Figure 3.1). The electromagnetic fields inside a waveguide satisfy the time-harmonic Maxwell's equations:

$$\text{(a) } \underline{\nabla} \times \underline{E} = j\omega\mu\underline{H} \qquad \text{(b) } \underline{\nabla} \cdot \epsilon\underline{E} = 0$$

$$\text{(c) } \underline{\nabla} \times \underline{H} = -j\omega\epsilon\underline{E} \qquad \text{(d) } \underline{\nabla} \cdot \mu\underline{H} = 0 \qquad (3.1)$$

where $\underline{E}$ is the electric field,

$\underline{H}$ is the magnetic field,

ϵ is the electric permittivity,

μ is the magnetic permeability.

A wave equation for $\underline{E}$ may be obtained by solving for $\underline{H}$ in (3.1a) and substituting this result into (3.1c) :

$$\underline{\nabla} \times \frac{1}{\mu} \underline{\nabla} \times \underline{E} - k_0^2 \epsilon_r \underline{E} = 0, \tag{3.2}$$

where k_0 is the free-space wave number $(\frac{\omega}{c})$.

An equivalent wave equation may be obtained for $\underline{H}$.

Assuming translational symmetry along the z-direction, as in Figure 3.1, the electric field may be written as :

$$E(x,y,z) = [\underline{E}_t(x,y) + \underline{E}_z(x,y)]e^{\pm j\beta z}, \tag{3.3}$$

where $\underline{E}_t$ is the component of $\underline{E}$ normal to $\underline{a}_z$

$\underline{E}_z$ is the component of $\underline{E}$ parallel to $\underline{a}_z$

If ϵ and μ are uniform, the tranverse electric field at port p can be Fourier-decomposed in terms of TE and TM harmonics :

$$\underline{E}_t = \sum_{m=1}^{\infty} V_m \underline{e}_m + \sum_{m=1}^{\infty} V'_m \underline{e}'_m, \tag{3.4}$$

where $V_m = \iint_{\partial\Omega_p} \underline{E}_t \cdot \underline{e}_m \, dS$

$V'_m = \iint_{\partial\Omega_p} \underline{E}_t \cdot \underline{e}'_m \, dS$

$\underline{e}_m$ is the electric field of the m^{th} TE mode

$\underline{e}'_m$ is the electric field of the m^{th} TM mode

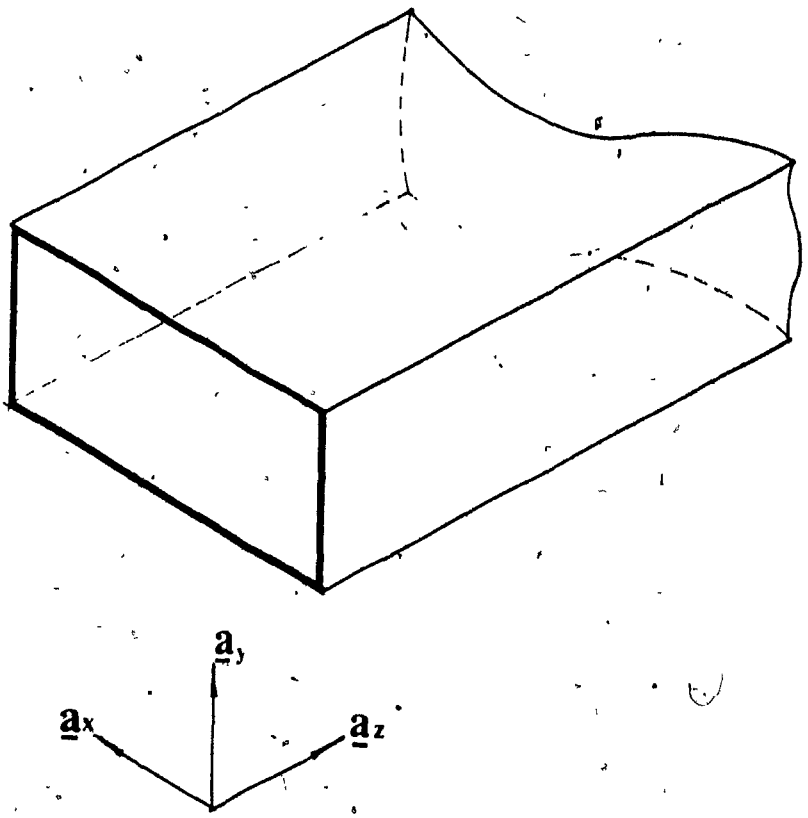

FIG 3.1 A HOLLOW RECTANGULAR WAVEGUIDE

Similarly, the transverse magnetic field at port p may be expressed as :

$$\underline{H}_t = \sum_{m=1}^{\infty} I_m \underline{h}_m + \sum_{m=1}^{\infty} I'_m \underline{h}'_m, \tag{3.5}$$

where $I_m = \iint_{\partial\Omega_p} \underline{H}_t \cdot \underline{h}_m \, dS$

$I'_m = \iint_{\partial\Omega_p} \underline{H}_t \cdot \underline{h}'_m \, dS$

$\underline{h}_m$ is the magnetic field of the $m^{th} TE$ mode

$\underline{h}'_m$ is the magnetic field of the $m^{th} TM$ mode

Waveguides are usually driven at a frequency at which only the first TE mode propagates and all other modes are attenuated. In such a case, the propagation constant, β, in (3.3) is real and positive for the first TE mode and imaginary for all other modes. This is called single-mode operation of the waveguide.

3.2 - Waveguide Junctions

Figure 3.2 (see also Figure 1.2) depicts a structure at which several waveguides meet. Such a structure is called a waveguide junction. The junction may be considered an N-port circuit element by using the dominant-mode Fourier coefficients in (3.4) and (3.5), V_1 and I_1 to represent the voltage and current at a given port.

The coupling of energy from the different ports may be written, for example, as an admittance matrix relation:

$$\begin{pmatrix} I_1 \\ I_2 \\ \vdots \\ I_N \end{pmatrix} = \begin{pmatrix} Y_{11} & Y_{12} & \cdots & Y_{1N} \\ Y_{21} & Y_{22} & \cdots & Y_{2N} \\ \vdots & \vdots & \ddots & \vdots \\ Y_{N1} & Y_{N2} & \cdots & Y_{NN} \end{pmatrix} \cdot \begin{pmatrix} V_1 \\ V_2 \\ \vdots \\ V_N \end{pmatrix} \tag{3.6}$$

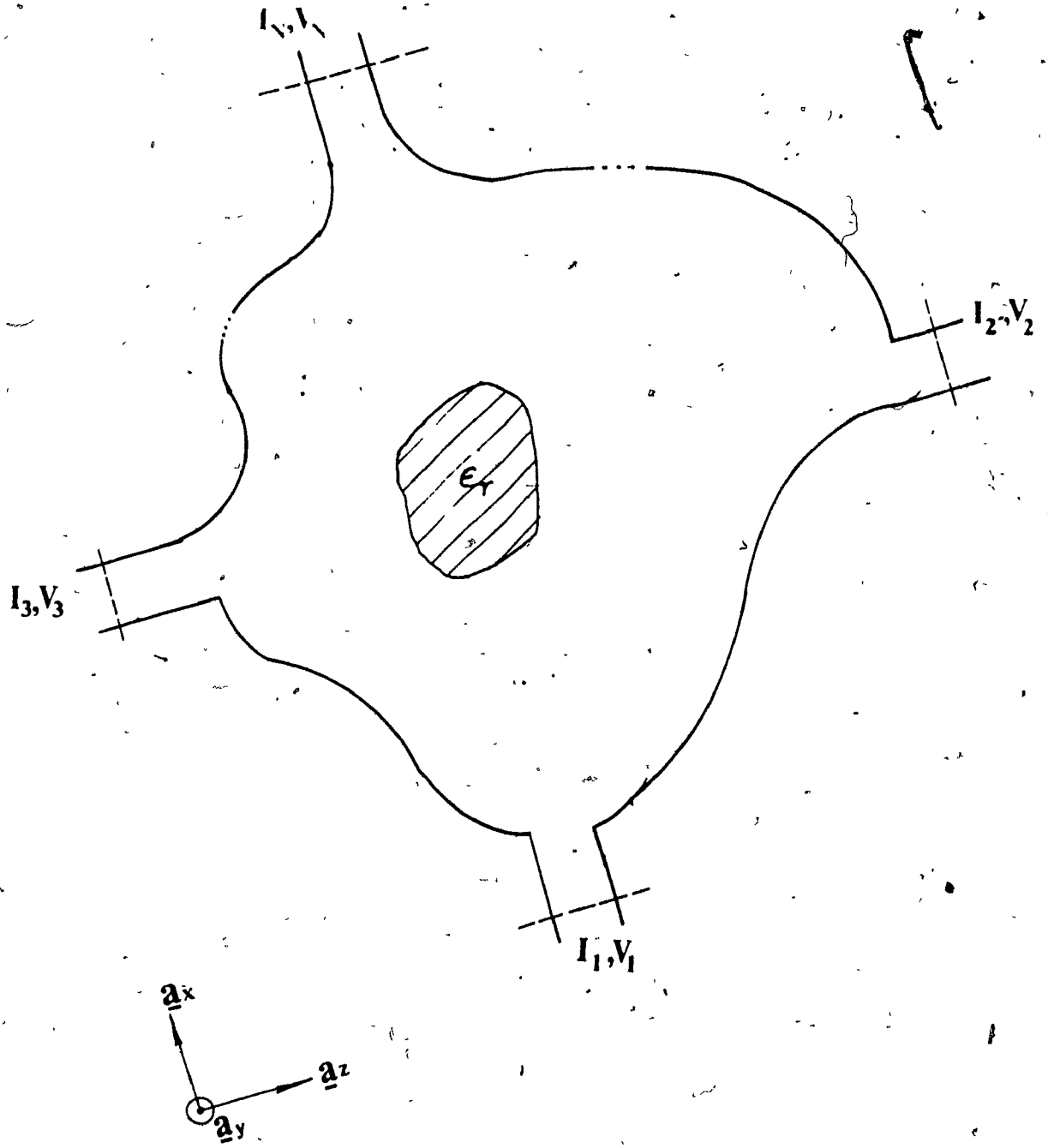

FIG 3.2 A WAVEGUIDE JUNCTION

(The mode subscripts in (3.4) and (3.5) have been dropped. The subscripts in (3.6) refer to the port numbers, instead.)

The admittance matrix characterises the coupling of energy in the dominant modes of each waveguide connected to the junction. The matrix allows the junction to be used in a lumped parameter circuit model.

3.3 - Determination of Network Parameters (Helszajn's Method [31])

In an N-port junction, the entries of the admittance or impedance matrix may be determined using open- and short-circuit experiments on pairs of ports. Figure 3.3(a) shows an N-port junction in which all but the i^{th} and j^{th} ports have been short-circuited. In Figure 3.3(b), Helszajn's equivalent circuit in terms of impedence parameters is presented. For symmetric junctions, the parameters are represented in Figure 3.3(c). The admittance parameters for this two-port may be obtained as follows :

step 1 – Short-circuit the terminal plane T and determine the impedance at P_i (z_s).

step 2 – Open-circuit the terminal plane T and determine the impedance at P_i (z_0).

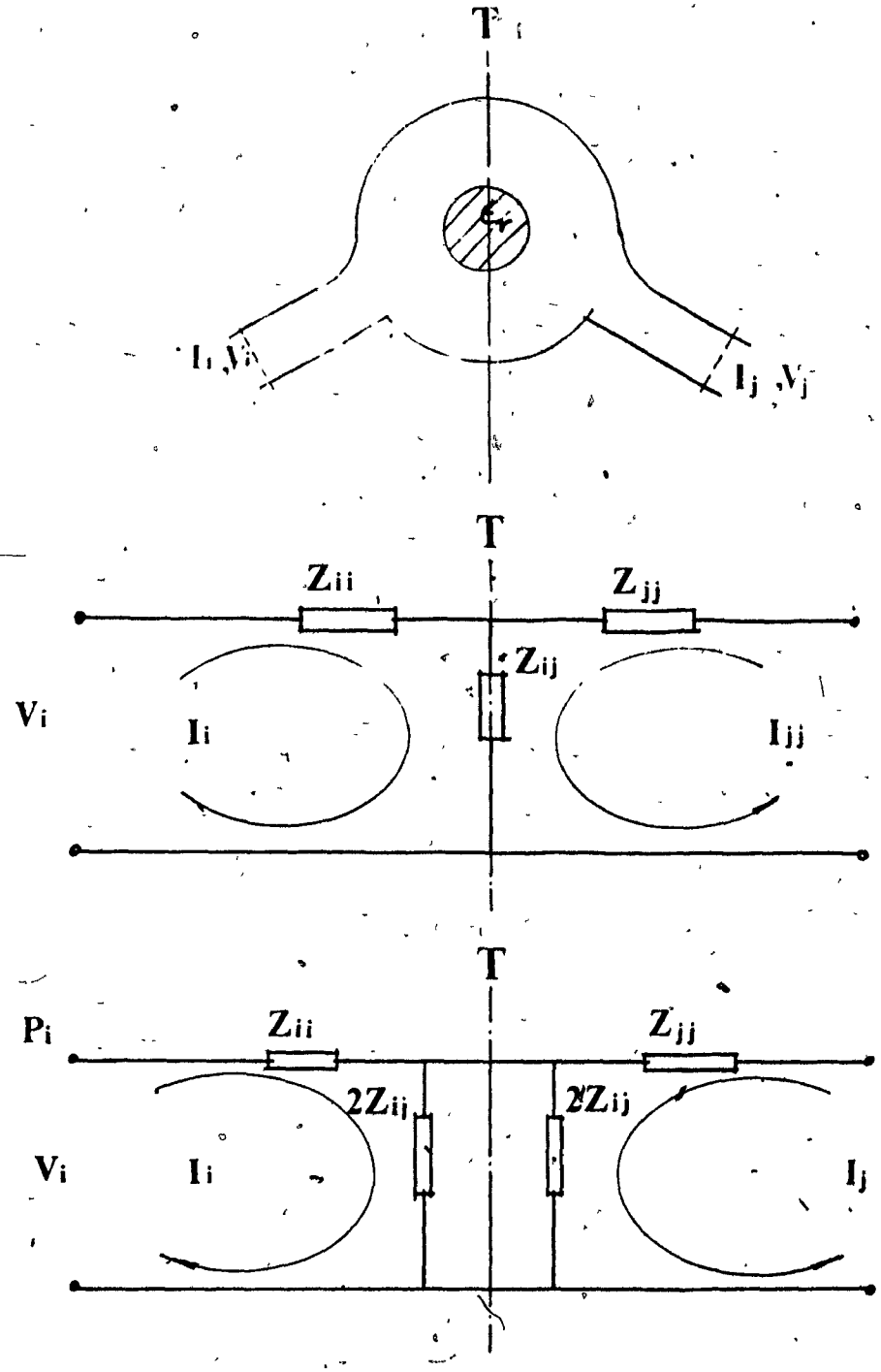

FIG 3.3 A SYMMETRIC TWO-PORT AND ITS EQUIVALENT CIRCUIT PARAMETERS

step 3 - Use Helszajn's model to extract impedance and admittance parameters:

$$
\begin{aligned}
z_{ii} &= z_a \\
z_{ij} &= \frac{z_0 - z_a}{2} \\
y_{ii} &= \frac{z_a}{z_a^2 - \frac{1}{4}(z_0 - z_a)^2} \\
y_{ij} &= \frac{z_a - z_0}{2z_a^2 - \frac{1}{2}(z_0 - z_a)^2}
\end{aligned}
\tag{3.7}
$$

Performing this analysis for each i,j-pair characterises the admittance matrix entirely. This experiment will be the basis for the formulation presented in Chapters 4 and 5.

3.4 - H-Plane Junctions

A special class of waveguide junctions is the H-plane junction. Consider the junction of Figure 1.2, in which conducting planes exist at $y = 0$ and at $y = b$, where b is the junction thickness. If the feeding waveguide dimensions are chosen so that the waveguide width, a, is larger than the waveguide thickness, b, then the TE_{m0} are the dominant modes of the waveguides. The electric field distributions of these modes have only a y-component and have no variation in the y-direction. As a result, the H-plane waveguide junction is amenable to a two-dimensional, scalar analysis. The H-plane waveguide geometry can be defined in two-dimensions, as in Figure 3.2 . For simplicity, the theory in the remainder of this chapter will deal with a two-dimensional junction, in which there is only single-mode operation of the feeding waveguides.

The electric field distributions of the TE_{m0} modes in rectangular waveguides

for single-mode operation are :

$$\underline{e}_m = A_m \sin \tfrac{m\pi x}{a} e^{-j\beta_m z} \underline{a}_y , \tag{3.8}$$

where $\beta_m = \sqrt{k_0^2 - \dfrac{m^2\pi^2}{a^2}}$

$=$ real for $m = 1$

$=$ imaginary for $m \geq 2$

The tangential magnetic field of the TE_{m0} modes is given by :

$$\underline{h}_m = y_m \underline{a}_z \times \underline{e}_m , \tag{3.9}$$

where y_m is the characteristic impedance of the TE_{m0} mode in the waveguide.

The voltages and currents at the plane $z = constant$, which cuts the waveguide, are:

$$V_p{}^m = \iint_{\partial\Omega_p} E_y \sin \tfrac{m\pi x}{a}\, dx\, dy$$

$$= b \int_{x=0}^{x=a} E_y \sin \tfrac{m\pi x}{a}\, dx \tag{3.10}$$

$$I_p{}^m = b \int_{x=0}^{x=a} H_x \sin \tfrac{m\pi x}{a}\, dx \tag{3.11}$$

These definitions for I and V will be used in Chapters 4 and 5.

3.5 - Summary

This Chapter presented some elctromagnetic theory needed for waveguide analysis. The waveguide junction, its representation, and the determination of its network parameters was discussed. Also, the special case of H-plane rectangular waveguides was presented.

Chapter 4 - Finite Element Waveguide Analysis

The finite element method may be used to extract waveguide network parameters [1][24][11][20][2][3][4][25] for arbitrarily-shaped junctions. The formulation common to all the references mentioned above will be referred to as the standard curl-curl formulation, and will be presented in this Chapter. The finite element theory will be presented for two-dimensional, scalar waveguide problems, where applicable. This formulation is appropriate for H-plane junction analysis.

4.1 - The Standard Curl-Curl Formulation

It has been demonstrated [24][26] that for a waveguide region, Ω in Figure 4.1, containing only lossless materials , the quantity :

$$F_0(\underline{E}) = \int_\Omega \left\{ \frac{1}{\mu_r} (\underline{\nabla} \times \underline{E})^2 - k_0^2 \epsilon_r \underline{E} \cdot \underline{E} \right\} d\Omega \qquad (4.1)$$

has a stationary point at $\underline{E} = \tilde{\underline{E}}$, where $\tilde{\underline{E}}$ satisfies the curl-curl equation (3.2). It has been assumed here that both $\underline{E}$ and $\tilde{\underline{E}}$ satisfy the appropriate boundary conditions on $\partial\Omega$ (see Figure 4.1).

For H-plane junctions, $\underline{E} = E_v$ and Ω is an area rather than a volume. A scalar field approximation for $\underline{E}$, suitable for analysis of H-plane rectangular waveguide junctions, may be obtained by subdividing the region Ω into e triangular

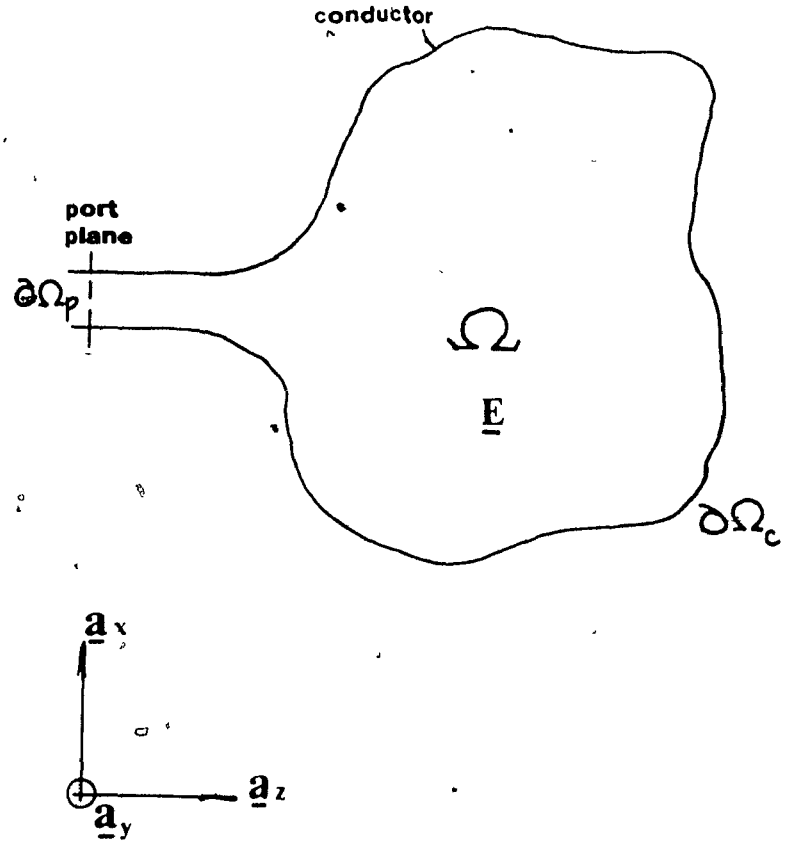

FIG 4.1 A ONE-PORT PROBLEM REGION

subregions such that (see Figure 4.2):

$$\Omega = \bigcup_{i=1} \Omega_i$$
$$\Omega_i \bigcap \Omega_j = \Omega_i \delta_{ij} \tag{4.2}$$

Within a given subregion, Ω_i, the approximate field may be expressed as a linear interpolation of the electric field values at the vertices (see Silvester[27]):

$$\underline{E}^{(i)} = E_v^{(i)} \underline{a}_v = \sum_{k=1}^{3} E_k \, \alpha_k(x,y) \quad \underline{a}_v \tag{4.3}$$

In finite element terminology, the vertices are called nodes and the triangular subregions, elements.

Inserting (4.3) into (4.1), the function may be written as a matrix quadratic form :

$$F_0(\underline{E}) = \underline{E}^T \mathbf{W} \underline{E} \tag{4.4}$$

where $\underline{E}$ is a column vector of E_i's

$\mathbf{W}$ is a square, symmetric matrix.

It may be shown that the stationary point of F_0, subject to the boundary conditions on $\underline{E}$, is $\underline{E}^*$, where:

$$\mathbf{W}' \underline{E}^* = \underline{R} \tag{4.6}$$

See Section 6.2 for details. The resulting solution vector, $\underline{E}^*$,may be used to approximate $\tilde{E}$ by interpolating between vertices in a given element using (4.3). This forms the basis of finite element theory.

4.2 - Waveguide Junction Admittance Parameters

Figure 4.3 illustates a waveguide junction in which all ports except port i have been open- or short-circuited and the ports have been defined to be far enough

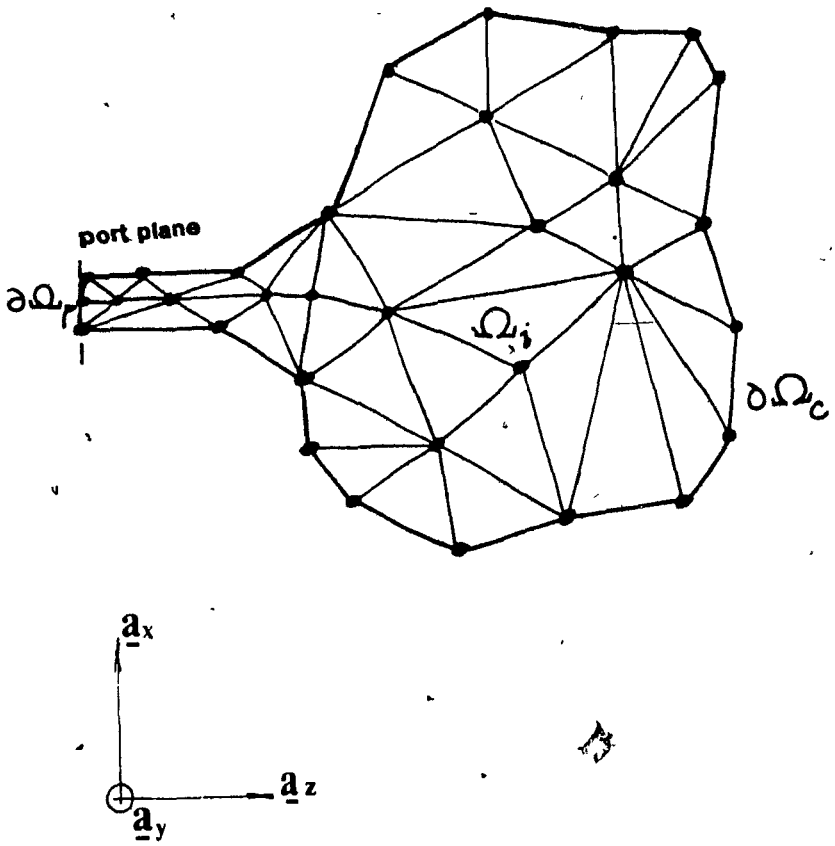

FIG 4.2 A DISCRETISED ONE-PORT WAVEGUIDE PROBLEM

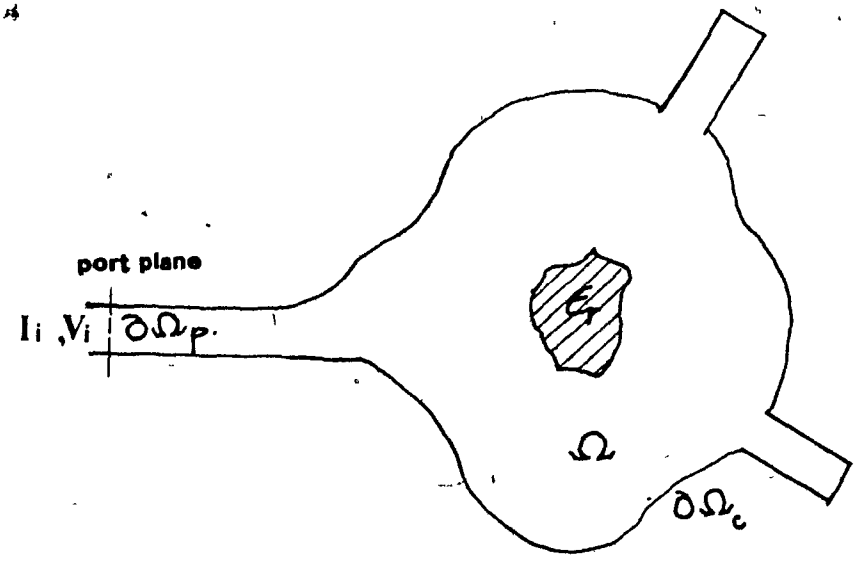

FIG 4.3 A TYPICAL PROBLEM TO ANALYSE

away from the junction cavity that evanescent modes of the waveguide have very little contribution to the fields at the port planes. In such a case, it has been demonstrated [24] that if port i is excited with a wave of unit voltage, then the admittance seen at port i is proportional to $F_0(\underline{\tilde{E}})$ (see Appendix I for proof) :

$$y = k \cdot F_0(\underline{\tilde{E}}) = k \int_\Omega \left\{ \frac{1}{\mu_r} (\underline{\nabla} \times \underline{E})^2 - k_0^2 \epsilon_r \underline{E} \cdot \underline{E} \right\} d\Omega, \qquad (4.7)$$

where k is a known constant.

Relation (4.7) allows the individual entries to be obtained using Helszajn's equivalent circuit models (Section 3.3) by performing open- and short-circuit experiments on pairs of ports. For a symmetric two-port, the procedure is

step 1 – Short-circuit the terminal plane T and solve the finite element problem corresponding to finding the stationary point of (4.1).

step 2 – Evaluate $y \approx k \cdot f_0(\underline{E}^*)$. Call this value y_s.

step 3 – Open-circuit the terminal plane T and obtain a finite element approximation of the admittance seen at plane P (y_0).

step 4 – Evaluate the diagonal and off-diagonal impedance and admittance

parameters:

$$z_{ii} = 1/y_s$$

$$z_{ij} = \frac{1/y_0 - 1/y_s}{2}$$

$$y_{ii} = \frac{1/y_s}{(1/y_s)^2 - \frac{1}{4}(1/y_0 - 1/y_s)^2} \tag{4.8}$$

$$y_{ij} = \frac{1/y_s - 1/y_0}{2(1/y_s)^2 - \frac{1}{2}(1/y_0 - 1/y_s)^2}$$

4.3 - Placement of the Junction Port Planes

There is a restriction imposed on the placement of port planes in the formulation above. In Figure 4.4, a portion of the waveguide junction is depicted. At port plane 1, the electric field may be written as :

$$\underline{E}_1 = c_1 \underline{e}_1 + c_2 \underline{e}_2 + \cdots + c_m \underline{e}_m + \cdots \tag{4.9}$$

where $\underline{e}_m$ is the electric field of the TE_{m0} mode. At port plane 2 the electric field is :

$$\underline{E}_2 = c_1 e^{-\Gamma_1 \Delta} \underline{e}_1 + c_2 e^{-\Gamma_2 \Delta} \underline{e}_2 + \cdots + c_m e^{-\Gamma_m \Delta} \underline{e}_m + \cdots + c_1' e^{+\Gamma_1 \Delta} \underline{e}_1 \tag{4.10}$$

If the dominant mode, TE_{10}, is the only propogating mode in the waveguide connected to the port, then Γ_1 is purely imaginary and all other Γ_i's are real and positive.

For large enough Δ, $e^{-\Gamma_m \Delta}$ is small for $m \geq 2$ so that electric field at plane

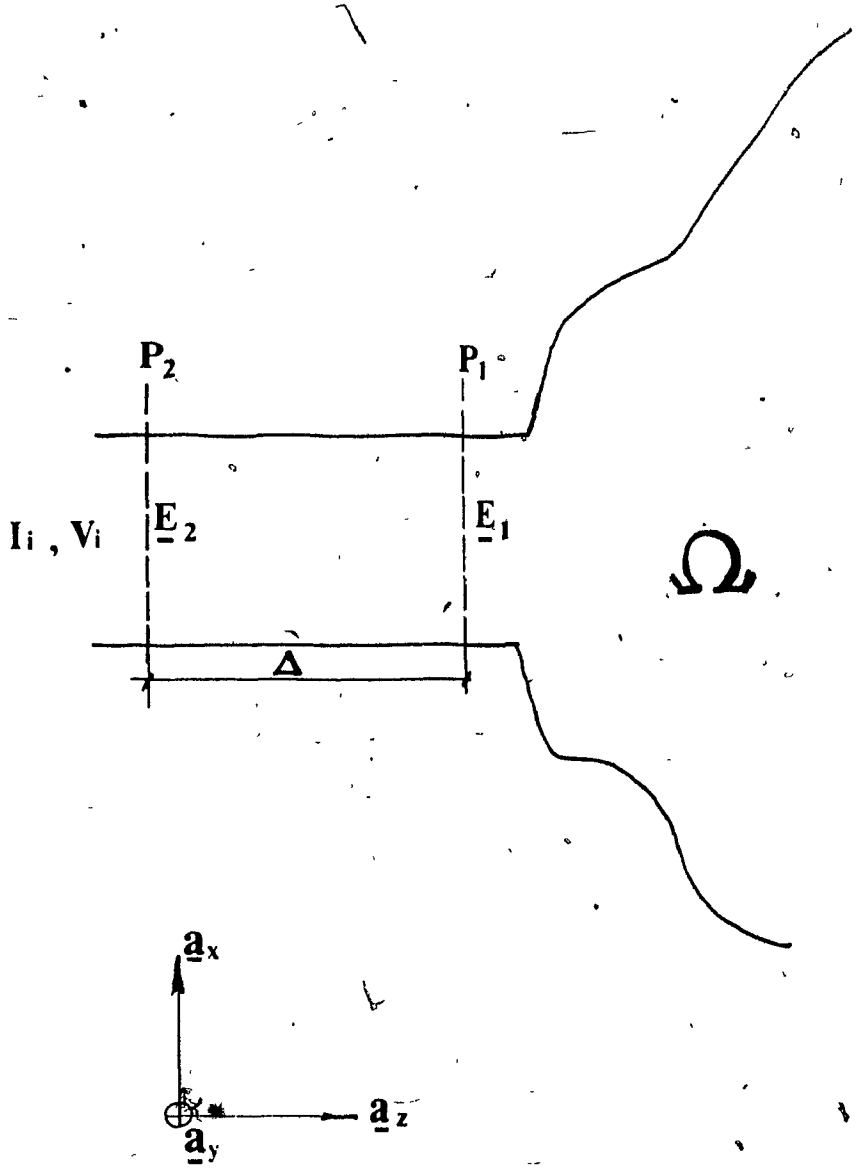

FIG 4.4 THE PORT PLANE AT PORT i

can be said to be comprised mainly of the dominant mode, $\underline{e}_1$:

$$E_2 \approx c_1 e^{-\Gamma_1 \Delta} \underline{e}_1 + c_1' e^{+\Gamma_1 \Delta} \underline{e}_1 \quad \text{for large} \quad \Delta \tag{4.11}$$

It is therefore justified, in such a case, to apply a Dirichlet boundary condition of the form :

$$\underline{E}_2 = \underline{e}_1 \tag{4.12}$$

in order to excite the port with a unit voltage TE_{10} wave.

The imposition of (4.12) is tantamount to imposing a non-homogeneous Dirichlet condition for the dominant mode and a homogeneous Dirichlet boundary condition for each of the higher TE_{m0} modes :

$$\begin{aligned} V_1 &= 1 \\ V_2 &= 0 \\ V_3 &= 0 \\ &\vdots \\ V_m &= 0, \\ &\vdots \end{aligned} \tag{4.13}$$

This method will be refered to as the Dirichlet port constraint method or "Dirichlet-port" method, for short. The above constraint does not, however, accurately model the fields of a true physical waveguide (where the higher-mode contributions are non-zero) unless the port plane is a large distance away from the junction. The true boundary value problem is effectively an open-boundary problem and the application of (4.12) is a virtual boundary condition that limits the problem region to a finite domain. The user of a formulation such as that described in this chapter is therefore restricted as to how close to the junction the port planes may be located.

4.4 - Summary

This chapter presented a finite element method to extract admittance parameters of an arbitrary-geometry H-plane waveguide junction. However, the port

planes of the junction must be situated sufficiently far from the junction cavity that the fields at these ports consist almost entirely of the dominant-mode fields. This restriction will be dealt with in the next chapter. chap5

Chapter 5 - A New Finite Element Method for Waveguide Analysis

The need to account for evanescent modes at the planes of the ports of a waveguide junction has been mentioned in many papers [16][2][3][4][25]. Two modifications to the method presented in the previous chapter are that:

(i) the energy-functional of equation (4.1) must be made to account for the energy contained in the higher waveguide modes, and

(ii) the input port boundary condition must be projective in nature, that is, it must only constrain the dominant - mode field component at the input port.

In order to accomplish these modifications, a new functional and some projective field operators must be developed. The theory will be presented in a three-dimensional form. This type of analysis will allow extensions of the theory to problems other than the H-plane junctions presented in this thesis. The theory will assume single-mode operation of the feeding waveguides throughout.

5.1 - Projective Operators and a New Functional

The electric field contribution from the m^{th} TE mode, $\underline{e}_m$, at a given waveguide junction port can be extracted from the electric field contribution, $\underline{E}$, by using

the following projection operator:

$$\mathbf{P}_m(\underline{E}) = \frac{\int_{\partial\Omega_p} \underline{E}\cdot\underline{e}_m \; d\Omega_p}{\int_{\partial\Omega_p} \underline{e}_m\cdot\underline{e}_m \; d\Omega_p} \quad \underline{e}_m \tag{5.1}$$

Given a port field distribution which is a mixture of several TE_{m0} modes, such as $\underline{E}_1$ of equation (4.9), the operator above extracts the m^{th} mode contribution so that:

$$\mathbf{P}_m(\underline{E}_1) = c_m e^{-\Gamma m \Delta} \underline{e}_m \tag{5.2}$$

For an evanescent mode ($m \geq 2$), the m^{th} mode magnetic field contribution is:

$$\mathbf{B}_m(\underline{E}) = b_m \underline{n} \times \mathbf{P}_m(\underline{E}) \tag{5.3}$$

where b_m is the characteristic susceptance of the TE_{m0} mode

$\underline{n}$ is a unit outward normal to the junction at the port boundary

$m \geq 2$

The total higher mode ($m = 2, 3, ...$) contribution to the magnetic field is given by:

$$\overline{\mathbf{B}}_1(\underline{E}) = \sum_{m=2}^{\infty} \mathbf{B}_m(\underline{E}) \tag{5.4}$$

By analogy, the projection operators $\mathbf{Q}_m(\underline{H})$ and $\overline{\mathbf{Q}}_1(\underline{H})$ can be defined such that:

$$\mathbf{Q}_m(\underline{H}) = \frac{\int_{\partial\Omega_p} \underline{H}\cdot\underline{h}_m \; d\Omega_p}{\int_{\partial\Omega_p} \underline{h}_m\cdot\underline{h}_m \; d\Omega_p} \quad \underline{h}_m$$

and

$$\overline{\mathbf{Q}}_1(\underline{H}) = \sum_{m=2}^{\infty} \mathbf{Q}_m(\underline{H})$$

The operators in (5.1), (5.3), and (5.4) are useful in developing a new functional and a new form of the boundary conditions needed in waveguide analysis. The

functional, $F_0(\underline{E})$, in equation (4.1) is proportional to the time-average outward-going power in the junction. This may be related to port admittances through the application of Poynting's Theorem (see Appendix I for proof). The time-average outward-going power in the TE_{10} mode is given by:

$$F(\underline{E}) = F_0(\underline{E}) + k_0\eta_0 \int_{\partial\Omega_p} \overline{\mathbf{B}}_1(\underline{E}) \times \underline{E} \cdot \underline{n}\, d\Omega_p \qquad (5.5)$$

The surface term above represents the outward-going power contained in the higher ($m \geq 2$) modes. The quantity may be used as a functional similar to the functional $F_0(\underline{E})$. This will be shown in the following sections.

The boundary condition on the first mode of the waveguide at $\partial\Omega_p$ can be written as:

$$\mathbf{P}_1(\underline{E}) = \underline{e}_1$$

for the first mode and for each higher mode, by application of equation (5.3):

$$\overline{\mathbf{Q}}_1(\frac{1}{j\omega\mu}\underline{\nabla} \times \underline{E}) = \overline{\mathbf{B}}_1(\underline{E}).$$

A justification for the above relation may be made as follows. $\overline{\mathbf{Q}}_1(\underline{H})$ is the higher-mode component of the magnetic field at the port and $\overline{\mathbf{B}}_1(\underline{E})$ is the evanescent portion of the magnetic field, assuming only outwardly-decaying higher modes. For single-mode operation, $\overline{\mathbf{Q}}_1(\underline{H})$ must equal $\overline{\mathbf{B}}_1(\underline{E})$.

The above two conditions provide adequate constraint for proper problem specification. This method of imposing the unit-voltage condition is called the "projective-port" method.

5.2 - The Stationary Point of $F(\underline{E})$

Refering to Figure 4.2, consider a space, S, of functions, $\underline{E}$, defined in Ω such

that:

$$\underline{n} \times \underline{E} = 0 \qquad \text{on } \partial\Omega_c \text{ (conductor).,}$$

$$\text{and} \quad \mathbf{P}_1(\underline{E}) = \underline{e}_1 \qquad \text{unit voltage condition}$$

The following Theorem may be developed:

Theorem A: If $\tilde{\underline{E}}$ is the stationary point of $F(\underline{E})$ in S, then $\tilde{\underline{E}}$ satisfies the curl-curl equation and the evanescent mode condition:

$$\overline{\mathbf{Q}}_1(\tilde{\underline{H}}) = \overline{\mathbf{B}}_1(\tilde{\underline{E}}).$$

Proof

The first variation of the functional, $F(\underline{E})$, with respect to an arbitrary function $\underline{u}$, which satisfies homogeneous boundary conditions on $\partial\Omega$ and $\mathbf{P}_1(\underline{u}) = 0$ on $\partial\Omega_p$ is:

$$\delta F(\tilde{\underline{E}}), \underline{u} = \int_\Omega \left\{ \frac{2}{\mu_r}(\nabla \times \tilde{\underline{E}}) \cdot (\nabla \times \underline{u}) - 2k_0^2 \epsilon_r \tilde{\underline{E}} \cdot \underline{u} \right\} d\Omega + k_0 \eta_0 \int_{\partial\Omega_p} \left\{ \overline{\mathbf{B}}_1(\underline{u}) \times \tilde{\underline{E}} + \overline{\mathbf{B}}_1(\tilde{\underline{E}}) \times \underline{u} \right\} \cdot \underline{n}\, d\Omega_p$$

Applying the identity $\nabla \cdot (\underline{a} \times \underline{b}) = \underline{b} \cdot (\nabla \times \underline{a}) - \underline{a} \cdot (\nabla \times \underline{b})$,

$$\delta F(\tilde{\underline{E}}), \underline{u} = \int_\Omega \left\{ \frac{2}{\mu_r} \nabla \cdot (\underline{u} \times \nabla \times \tilde{\underline{E}}) + \frac{2}{\mu_r} \underline{u} \cdot \nabla \times \nabla \times \tilde{\underline{E}} - 2\epsilon_r k_0^2 \tilde{\underline{E}} \cdot \underline{u} \right\} \cdot \underline{n} d\Omega + 2k_0 \eta_0 \int_{\partial\Omega_p} \left\{ \overline{\mathbf{B}}_1(\tilde{\underline{E}}) \times \underline{u} \right\} \cdot \underline{n} d\Omega_p$$

Therefore,

$$\delta F(\tilde{\underline{E}}), \underline{u} = \int_\Omega \left\{ \frac{2}{\mu_r} \nabla \cdot (\underline{u} \times \nabla \times \tilde{\underline{E}}) \right\} \underline{n} d\Omega + 2k_0 \eta_0 \int_{\partial\Omega_p} \left\{ \overline{\mathbf{B}}_1(\tilde{\underline{E}}) \times \underline{u} \right\} \cdot \underline{n} d\Omega_p + \int_\Omega \frac{2}{\mu_r} \underline{u} \cdot (\nabla \times \nabla \times \tilde{\underline{E}} - k_0^2 \epsilon_r \tilde{\underline{E}}) \quad d\Omega$$

The Divergence Theorem can be applied to the first integral, above, to give:

$$\delta F(\tilde{\underline{E}}), \underline{u} = \int_{\partial\Omega} \frac{2}{\mu_r} \underline{u} \times \nabla \times \tilde{\underline{E}} \cdot \underline{n} d\Omega + 2k_0 \eta_0 \int_{\partial\Omega_p} \overline{\mathbf{B}}_1(\tilde{\underline{E}}) \times \underline{u} \cdot \underline{n} d\Omega_p + \int_\Omega \frac{2}{\mu_r} \underline{u} \cdot (\nabla \times \nabla \times \tilde{\underline{E}} - k_0^2 \epsilon_r \tilde{\underline{E}}) \quad d\Omega$$

Since $\underline{u} \times \underline{n} = \underline{E} \times \underline{n} = 0$ on conducting boundaries,

$$\delta F(\tilde{\underline{E}}), \underline{u} = \int_{\partial\Omega_p} \left\{ \frac{2}{\mu_r} \underline{u} \times \underline{\nabla} \times \tilde{\underline{E}} + 2k_0 \eta_0 \overline{\mathbf{B}}_1(\tilde{\underline{E}}) \times \underline{u} \right\} \cdot \underline{n} d\Omega_p$$
$$+ \int_\Omega \frac{2}{\mu_r} \underline{u} \cdot (\underline{\nabla} \times \underline{\nabla} \times \tilde{\underline{E}} - k_0^2 \epsilon_r \tilde{\underline{E}}) \quad d\Omega$$
$$= \int_{\partial\Omega_p} \left\{ 2\underline{u} \times \left[\frac{1}{\mu_r} \underline{\nabla} \times \tilde{\underline{E}} - k_0 \eta_0 \overline{\mathbf{B}}_1(\tilde{\underline{E}}) \right] \right\} \cdot \underline{n} d\Omega_p$$
$$+ \int_\Omega \frac{2}{\mu_r} \underline{u} \cdot (\underline{\nabla} \times \underline{\nabla} \times \tilde{\underline{E}} - k_0^2 \epsilon_r \tilde{\underline{E}}) \, d\Omega$$

$$\delta F(\tilde{\underline{E}}), \underline{u} = 2 \int_{\partial\Omega_p} (\underline{n} \times \underline{u}) \cdot \left[\frac{1}{\mu_r} \underline{\nabla} \times \tilde{\underline{E}} - k_0 \eta_0 \overline{\mathbf{B}}_1(\tilde{\underline{E}}) \right] d\Omega_p$$
$$+ \int_\Omega \frac{2}{\mu_r} \underline{u} \cdot (\underline{\nabla} \times \underline{\nabla} \times \tilde{\underline{E}} - k_0^2 \epsilon_r \tilde{\underline{E}}) \quad d\Omega$$

If $\tilde{\underline{E}}$ is a stationary point of $F(\underline{E})$, then the volume and surface integrals above must each vanish seperately. This implies that:

$$\underline{\nabla} \times \underline{\nabla} \times \tilde{\underline{E}} - k_0^2 \epsilon_r \tilde{\underline{E}} = 0.$$

For $m = 1$ and $\underline{u} = \underline{e}_m$ on $\partial\Omega_p$, $\underline{n} \times \underline{u} = \frac{\underline{h}_m}{jb_m}$ and:

$$\delta F(\tilde{\underline{E}}), \underline{u} = \frac{2}{jb_m} \int_{\partial\Omega_p} \underline{h}_m \cdot \left[\frac{1}{\mu_r} \underline{\nabla} \times \tilde{\underline{E}} - k_0 \eta_0 \overline{\mathbf{B}}_1(\tilde{\underline{E}}) \right] d\Omega_p = 0$$

From the definition of $\mathbf{Q}_m(\cdot)$, this implies that:

$$\overline{\mathbf{Q}}_1 \left[\frac{1}{\mu_r} \underline{\nabla} \times \tilde{\underline{E}} - k_0 \eta_0 \overline{\mathbf{B}}_1(\tilde{\underline{E}}) \right] = 0$$

And since $\overline{\mathbf{Q}}_1(\overline{\mathbf{B}}_1(\tilde{\underline{E}})) = \overline{\mathbf{B}}_1(\tilde{\underline{E}})$,

$$\overline{\mathbf{Q}}_1 \left(\frac{1}{\mu_r} \underline{\nabla} \times \tilde{\underline{E}} \right) = \overline{\mathbf{B}}_1(\tilde{\underline{E}})$$

which is the evanescent mode condition.

Therefore, $\tilde{\underline{E}}$ satisfies the curl-curl equation as well as the evanescent mode condition.

Therefore, as the above proof demonstrates, the solution field, $\underline{\tilde{E}}$, which satisfies the curl-curl equation may be found by using the functional $F(\underline{E})$ instead of $F_0(\underline{E})$ and by applying $\mathbf{P}_1(\underline{E}) = \underline{e}_1$ instead of $\underline{E} = \underline{e}_1$ on the port boundary in a variational formulation similar to that presented in Chapter 4. The higher modes at the port plane have been accounted for and, therefore, there is no restriction whatever on the distance that the planes must be from the port, unlike the standard formulation.

5.3 - The Physical Significance of $F(\underline{\tilde{E}})$

In addition to the similarity in the stationarity properties of $F(\underline{E})$ and $F_0(\underline{E})$ presented above, the two functionals also share similar properties when evaluated at their respective stationary points. The following Theorem applies to $F_0(\underline{\tilde{E}})$:

Theorem B: $F(\underline{E})$ is proportional to the admittance seen at port $\partial\Omega_p$

Proof:

Since:

$$\underline{\nabla} \cdot (\underline{a} \times \underline{b}) = \underline{b} \cdot (\underline{\nabla} \times \underline{a}) - \underline{a} \cdot (\underline{\nabla} \times \underline{b}),$$

then:

$$(\underline{\nabla} \times \underline{\tilde{E}}) \cdot (\underline{\nabla} \times \underline{\tilde{E}}) = \underline{\nabla} \cdot (\underline{\tilde{E}} \times \underline{\nabla} \times \underline{\tilde{E}}) + \underline{\tilde{E}} \cdot (\underline{\nabla} \times \underline{\nabla} \times \underline{\tilde{E}})$$

$$F(\underline{\tilde{E}}) = \int_\Omega \left(\frac{1}{\mu_r} \left[\underline{\nabla} \cdot (\underline{\tilde{E}} \times \underline{\nabla} \times \underline{\tilde{E}}) + \underline{\tilde{E}} \cdot (\underline{\nabla} \times \underline{\nabla} \times \underline{\tilde{E}}) \right] - k_0^2 \epsilon_r \underline{\tilde{E}}^2 \right) d\Omega + k_0 \eta_0 \int_{\partial\Omega_p} \overline{\mathbf{B}}_1(\underline{\tilde{E}}) \times \underline{\tilde{E}} \cdot \underline{n} d\Omega_p$$

$$F(\underline{\tilde{E}}) = \int_\Omega \underline{\nabla} \cdot (\underline{\tilde{E}} \times \frac{1}{\mu_r} \underline{\nabla} \times \underline{\tilde{E}}) d\Omega + \int_\Omega \frac{1}{\mu_r} \underline{\tilde{E}} \cdot (\underline{\nabla} \times \underline{\nabla} \times \underline{\tilde{E}}) d\Omega - k^2 \int_\Omega \epsilon_r \underline{\tilde{E}}^2 d\Omega + k_0 \eta_0 \int_{\partial\Omega_p} \overline{\mathbf{B}}_1(\underline{\tilde{E}}) \times \underline{\tilde{E}} \cdot \underline{n} d\Omega_p$$

$$F(\underline{\tilde{E}}) = \int_{\partial\Omega} (\underline{\tilde{E}} \times \frac{1}{\mu_r} \underline{\nabla} \times \underline{\tilde{E}}) \cdot \underline{n} \, d\Omega + k_0 \eta_0 \int_{\partial\Omega_p} \overline{\mathbf{B}}_1(\underline{\tilde{E}}) \times \underline{\tilde{E}} \cdot \underline{n} d\Omega_p$$

Now the first integral is zero everywhere except at the ports.

$$F(\underline{\tilde{E}}) = \int_{\partial\Omega_p} (\underline{\tilde{E}} \times \frac{1}{\mu_r}\underline{\nabla} \times \underline{\tilde{E}}) \cdot \underline{n}\, d\Omega_p + k_0\eta_0 \int_{\partial\Omega_p} \overline{\mathbf{B}}_1(\underline{\tilde{E}}) \times \underline{\tilde{E}} \cdot \underline{n}\, d\Omega_p$$

$$F(\underline{\tilde{E}}) = \int_{\partial\Omega_p} \underline{\tilde{E}} \times \left[\frac{1}{\mu_r}\underline{\nabla} \times \underline{\tilde{E}} - k_0\eta_0 \overline{\mathbf{B}}_1(\underline{\tilde{E}})\right] \cdot \underline{n}\, d\Omega_p$$

Now the fields can be written at the ports as follows:

$$\underline{\tilde{E}}_t = \underline{e}_1 + \sum_{m=2}^{\infty} V_m \underline{e}_m$$

$$\underline{\tilde{H}}_t = I_1 \underline{h}_1 + \sum_{m=2}^{\infty} I_m \underline{h}_m$$

and for each mode m of the port waveguide:

$$\underline{h}_m = -y_m \underline{n} \times \underline{e}_m$$

$$\Rightarrow \underline{\tilde{H}}_t = -I_1 y_1 \underline{n} \times \underline{e}_1 - \sum_{m=2}^{\infty} I_m y_m \underline{n} \times \underline{e}_m$$

And for outward-going evanescent modes:

$$V_m = -I_m$$

$$\Rightarrow \underline{\tilde{H}}_t = -I_1 y_1 \underline{n} \times \underline{e}_1 + \sum_{m=2}^{\infty} V_m y_m \underline{n} \times \underline{e}_m$$

From Maxwell's equations:

$$\underline{\tilde{H}} = -\frac{1}{j\omega\mu_0\mu_r}\underline{\nabla} \times \underline{\tilde{E}} = j\frac{1}{\eta_0 k_0 \mu_r}\underline{\nabla} \times \underline{\tilde{E}}$$

we can thus write:

$$\frac{1}{\mu_r}\underline{\nabla} \times \underline{\tilde{E}} = -jk_0\eta_0\underline{\tilde{H}}$$

$$\Rightarrow F(\underline{\tilde{E}}) = \int_{\partial\Omega_p} \underline{\tilde{E}} \times \left[-jk_0\eta_0\underline{\tilde{H}} - k_0\eta_0\overline{\mathbf{B}}_1(\underline{\tilde{E}})\right] \cdot \underline{n}\, d\Omega_p$$

$$F(\underline{\tilde{E}}) = \int_{\partial\Omega_p} \underline{\tilde{E}} \times \left[-jk_0\eta_0\left(-I_1 y_1 \underline{n} \times \underline{e}_1 + \sum_{m=2}^{\infty} V_m y_m \underline{n} \times \underline{e}_m\right)\right.$$

$$\left. - k_0\eta_0\overline{\mathbf{B}}_1(\underline{\tilde{E}})\right] \cdot \underline{n}\, d\Omega_p$$

Now

$$-k_0\eta_0\overline{\mathbf{B}}_1(\tilde{\underline{E}}) = -k_0\eta_0\underline{n}\times\sum_{q=2}^{\infty}b_q\mathbf{P}_q\left(\underline{e}_1+\sum_{m=2}^{\infty}V_m\,\underline{e}_m\right)$$

$$= -k_0\eta_0\underline{n}\times\sum_{m=2}^{\infty}b_m\,V_m\,\underline{e}_m$$

$$F(\tilde{\underline{E}}) = \int_{\partial\Omega_p}\tilde{\underline{E}}\times\Big[+jk_0\eta_0 I_1 y_1\,\underline{n}\times\underline{e}_1$$

$$- jk_0\eta_0\sum_{m=2}^{\infty}V_m\,y_m\,\underline{n}\times\underline{e}_m$$

$$+ k_0\eta_0\sum_{m=2}^{\infty}V_m\,b_m\,\underline{n}\times\underline{e}_m\Big]\cdot\underline{n}\;d\Omega_p$$

$$= jk_0\eta_0\int_{\partial\Omega_p}\tilde{\underline{E}}\times I_1\,y_1\,\underline{n}\times\underline{e}_1\cdot\underline{n}\;d\Omega_p$$

$$= -I_1 b_1 k_0\eta_0\int_{\partial\Omega_p}\tilde{\underline{E}}\times(\underline{n}\times\underline{e}_1)\cdot\underline{n}\;d\Omega_p$$

$$= -I_1 b_1 k_0\eta_0\int_{\partial\Omega_p}\Big[\underline{n}(\tilde{\underline{E}}\cdot\underline{e}_1)-\underline{e}_1(\tilde{\underline{E}}\underline{n})\Big]\cdot\underline{n}\;d\Omega_p$$

$$= -I_1 b_1 k_0\eta_0\int_{\partial\Omega_p}\tilde{\underline{E}}\cdot\underline{e}_1\;d\Omega$$

But

$$\mathbf{P}_1(\tilde{\underline{E}}) = \underline{e}_1 \quad , \quad \text{on} \quad \partial\Omega_p$$

$$\underline{e}_1\frac{\int_{\partial\Omega_p}\tilde{\underline{E}}\cdot\underline{e}_1\,\partial\Omega_p}{\int_{\partial\Omega_p}\underline{e}_1^2\,\partial\Omega_p} = \underline{e}_1 \qquad \text{on} \quad \partial\Omega_p$$

so

$$F(\tilde{\underline{E}}) = -I_1 b_1 k_0\eta_0\int_{\partial\Omega_p}\underline{e}_1^2\;d\Omega$$

$$F(\tilde{\underline{E}}) \propto I_1$$

Therefore, as with the standard method , port admittances may be obtained from the evaluation of the new functional at its stationary point.

5.4 - Positive Definite Properties of $F(\underline{E})$

The functional, $F(\underline{E})$, may be shown to be positive definite under certain conditions (see Appendix II for some background in numerical analysis and a proof of the positive definite properties of the functional). Under these conditions, one may obtain a faster solution of the finite element matrix equation. Once the functional, $F(\underline{E})$, has been has been shown to be positive definite , the discretised operator may be written in matrix form:

$$F(\underline{E}) = \underline{E}^T \mathbf{W} \underline{E} \tag{5.6}$$

where $\mathbf{W}$ is positive definite. The stationary point of $F(\underline{E})$, subject to the port consraint, $\mathbf{P}_i(\underline{E}) = \underline{e}_i$, is a solution to the matrix equation (see Section 6.2):

$$\mathbf{W}'' \underline{E} = \underline{R} \tag{5.7}$$

where $\mathbf{W}''$ is also positive definite. The matrix equation above can be solved very efficiently by performing an incomplete Cholesky decomposition of $\mathbf{W}''$ and subsequently applying the conjugate gradient method to solve for $\underline{E}$. If $F(\underline{E})$ is not positive definite, then neither is $\mathbf{W}''$ and an alternate method must be used, such as symmetric Gaussian elimination. The time saved by exploiting positive definiteness may be significant for large problems since the conjugate gradient method requires $O(N^{\frac{3}{2}})$ operations whereas a symmetric Gaussian solver requires $O(N^2)$ operations, where N is the dimensionality of the matrix (Kershaw [30]). Therefore, to summarize the above results and those from Appendix II:

> A faster solution to the finite element matrix in equation (5.7) may be obtained if the driving frequency , k_0, is smaller than the lowest resonant frequency of the closed cavity, Ω, in Figure 4.2.

5.5 - Summary

A new finite element formulation was presented in this Chapter with the following properties:

(i) The new fomulation can be used to obtain waveguide admittances for H - plane junctions.

(ii) The formulation is free of the port restriction found in , for example, Webb[1].

(iii) The operator problem resulting from the new formulation is positive definite for some ranges of the driving frequency, resulting in faster matrix solution times.

Chapter. 6 - Implementation and Results

This Chapter is divided into two parts: Part I will discuss the implementation of the finite element method presented in Chapter 5. Part II will present results that validate the theory presented in earlier chapters.

PART I - IMPLEMENTATION

This Part will present an algorithm for extracting the admittance parameters of an H-plane waveguide junction.

6.1 - Matrix Assembly

The assembly of the global finite element matrix can be divided into two tasks: (i) the standard functional assembly, (F_0), and (ii) the port boundary term assembly (refer to equations (5.4) and (5.5)).

The contribution to F_0 from an arbitrary element k is:

$$F_0^{(k)}(\underline{E}) = \int_{\Omega_k} \frac{1}{\mu_k}(\underline{\nabla} \times \underline{E})^2 \, d\Omega_k - k_0^2 \epsilon_k \int_{\Omega_k} \underline{E} \cdot \underline{E} \, d\Omega_k \qquad (6.1)$$

where Ω_k is the region represented by element k,

μ_k is the relative permeability in element k,

ϵ_k is the relative permittivity in element k.

Substituting $\underline{E} = \sum_{i=1}^{3} E_i \alpha_i(x,z)\underline{a}_y$

$$F_0^{(k)}(\underline{E}) = \underline{E}^{(k)} \mathbf{W}_0^{(k)} \underline{E}^{(k)}, \tag{6.2}$$

where $\mathbf{W}_0^{(k)}(i,j) = \int_{\Omega_k} \left\{ \frac{1}{\mu_k} (\underline{\nabla}\alpha_i) \cdot (\underline{\nabla}\alpha_j) - k_0^2 \epsilon_r \alpha_i \cdot \alpha_j \right\} d\Omega_k$

and $\underline{E}^{(k)}$ is a 3-vector of nodal electric field y-components in element k. The global matrix, $\mathbf{W}_0$, is constructed by mapping the local indices for element k into global indices so that:

$$F_0(\underline{E}) = \sum_{k=1}^{n_e} F_0(\underline{E}) = \underline{E}^T \mathbf{W}_0 \underline{E} \tag{6.3}$$

where n_e is the number of elements.

The port boundary term of $F(\underline{E})$ may be constructed by considering all nodes which define the port boundary as being part of a large "port element". Figure 6.1(a) depicts the nodes defining the port element and shows the port coordinate system. Figure 6.1(b) presents two arbitrary tent-functions, used as first order finite element trial functions for the assembly of the port term. Writing $\underline{E}$ along the port as:

$$\underline{E} = \sum_{n=1}^{n_p} \underline{E}_n \alpha_n \underline{a}_y \tag{6.4},$$

where n_p is the number of port nodes. The boundary term may now be expressed as:

$$\begin{aligned} \text{boundary} \quad \text{term} &= \sum_{m=2}^{\infty} b_m \sum_{i=1}^{n_p} \sum_{j=1}^{n_p} E_i E_j K_i^m K_i^m \\ &= \sum_{m=2}^{\infty} b_m \underline{E}^T \mathbf{W}_m \underline{E}, \end{aligned} \tag{6.5}$$

where K_i^m is a function which depends on the port coordinate of node i (see Appendix III).

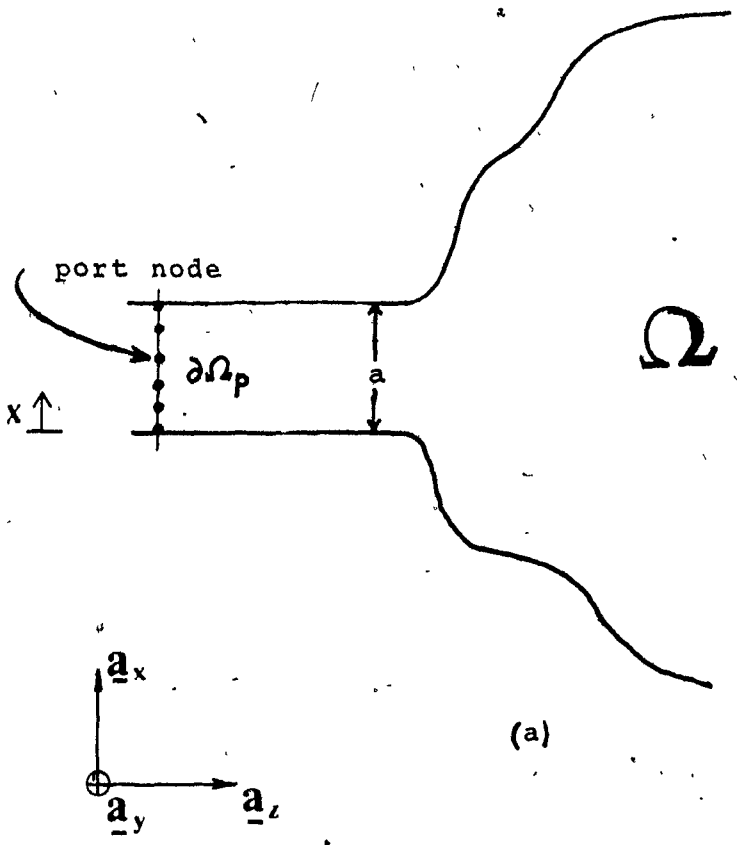

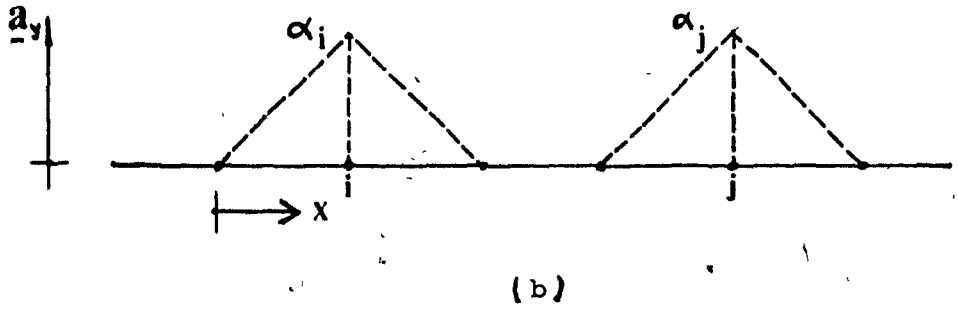

FIG 6.1 (a) The Port Boundary And Coordinate, x
(b) Two Arbitrary Port Trial Functions

The functional can now be written as:

$$F(\underline{E}) = \underline{E}^T \mathbf{W}_0 \underline{E} + \sum_{m=2}^{\infty} \underline{E}^{(p)T} \mathbf{W}_m^{(p)} \underline{E}^{(p)} \qquad (6.6)$$
$$= \underline{E}^T \mathbf{W} \underline{E}$$

The matrix, W, is the global finite element operator matrix.

6.2 - Matrix Modification

In order to obtain the solution vector, $\underline{E}^*$, the functional in equation (6.6) must be rendered stationary with respect to $\underline{E}$, subject to two special conditions. The first condition is that at electrical conductor boundaries:

$$E_i = 0 \quad \text{if node } i \text{ is on a conductor.} \qquad (6.7)$$

The second condition imposed upon $\underline{E}$ is that the field at the port plane must represent that of a unit voltage excitation. This may be enforced on the problem by applying the condition:

$$\mathbf{P}_1(\underline{E}) = \underline{e}_1 = A \sin \frac{\pi x}{a} \underline{a}_y \qquad (6.8)$$

where A is chosen so that the input wave carries unit power. Equation (6.8) may be written in the following form:

$$\sum_{i=1}^{N} \eta_i E_i = 1 \qquad (6.9)$$

where η_i is a weight arising from the operator $\mathbf{P}_1$ (see Appendix III). The discretised form of $F(\underline{E})$ can be modified to account for the two constraints. The first modification accounts for the short-circuit condition (6.7):

$$\mathbf{W}' \underline{E} = 0 \quad \text{where} \qquad (6.10)$$

$$W'(i,j) = \begin{cases} W(i,j) & \text{if } i,j \in V \\ 0 & \text{if } i \text{ or } j \in P \text{ and } i \neq j \\ 1 & \text{if } i = j \in P \end{cases} \tag{6.11}$$

V is the set of all free (unconstrained) nodes.

P is the set of all nodes on the conducting boundaries.

The zero righthand side results from the application of homogeneous boundary conditions due to the conducting boundaries. The matrix $\mathbf{W}'\underline{E} = 0$ may be further modified to account for condition (6.11) (see Webb[29] for details), leading to the stationarity condition:

$$\mathbf{W}''\underline{E} = \underline{R}, \tag{6.12}$$

where:

$$R_i = \frac{c}{\eta_m} W'(i,m) + \frac{\eta_i}{\eta_m^2} W'(m,m) + k\eta_i$$

$$W''(i,j) = W'(i,j) - \frac{\eta_i}{\eta_m} W'(m,j) - \frac{\eta_j}{\eta_m} W'(m,i) + \frac{\eta_i \eta_j}{\eta_m^2} W'(m,m) + k\eta_i\eta_j$$

m is an index chosen so that $\eta_m \neq 0$

k is an arbitrary constant > 0

The final matrix relation of equation (6.12) leads directly to obtaining the solution vector, $\underline{E}^*$.

6.3 - Matrix Equation Solution

If the waveguide junction must be analysed over a large range of frequencies, then it is advantageous to exploit the positive definite properties of $\mathbf{W}''$. This may be accomplished by implementing the structure in Figure 6.2. Note that for positive definite frequency ranges of $\mathbf{W}''$ the conjugate gradient (CG) method may be used to solve the matrix equation (see Kershaw [30] for CG and ICCG method details). For indefinite ranges a symmetric Gaussian elimination solver may be used. This structure makes optimal use of the positive properties of $\mathbf{W}''$.

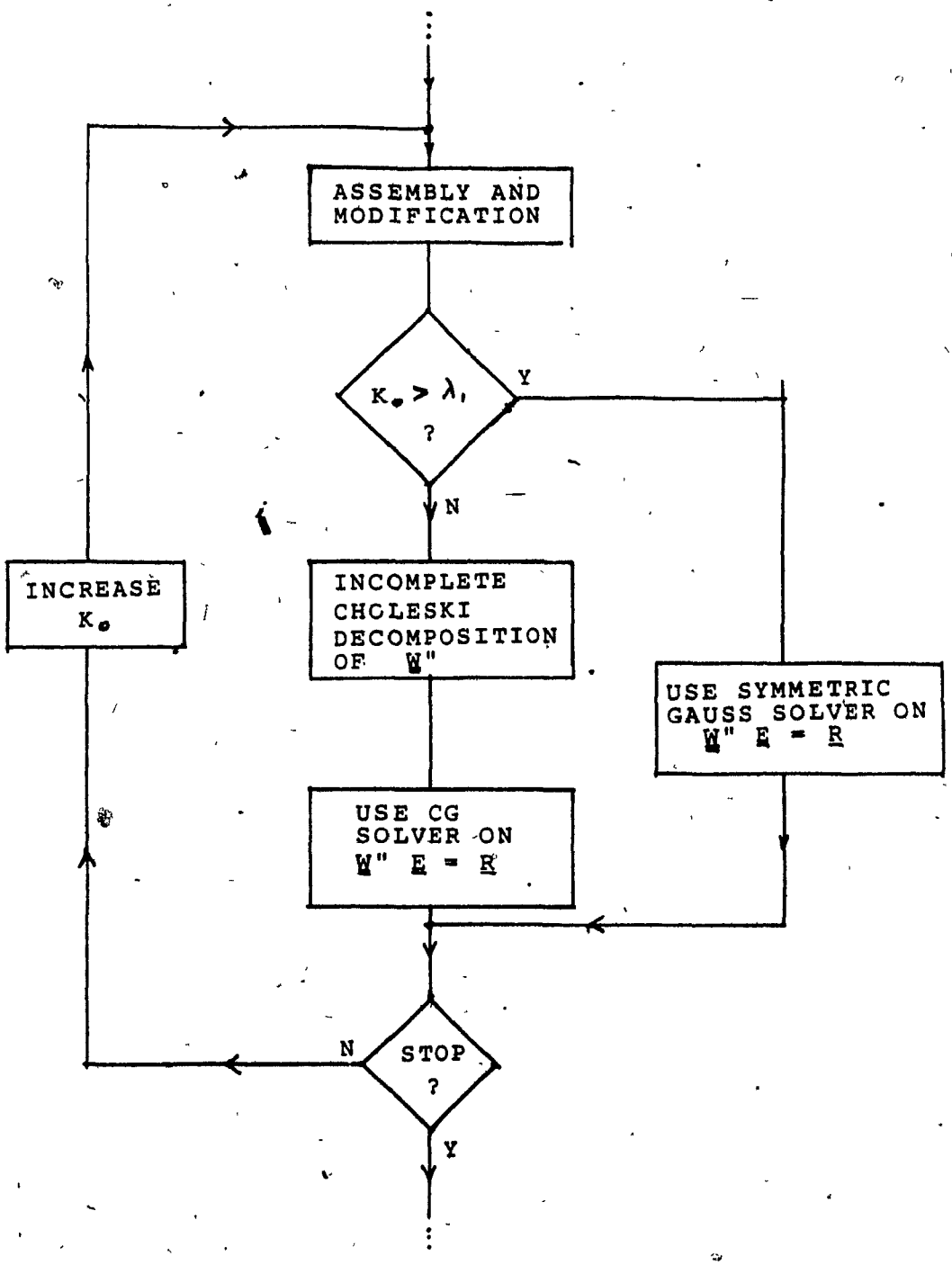

FIG 6.2 A FLOW DIAGRAM THAT EXPLOITS THE POSITIVE DEFINITE PROPERTY OF $\underline{\underline{W}}''$, WHEN POSSIBLE

6.4 - The Program

The implementation described above was programmed in FORTRAN-77 on a Digital Equipment Microvax II, running Unix V1.2. The problem geometry data was defined using MAGMESH, a well-known interactive finite element modeler. The solution structure described in Section 6.3 was not implemented. Instead, a symmetric Gauss solver was used for all ranges of frequency, k_0, for simplicity. Results of this program are presented in Part II of this Chapter.

PART II - RESULTS

6.5 - The Empty Waveguide Stub

As a first test of the program described in the previous section, an empty, short-circuited waveguide was analysed. The waveguide one-port junction is depicted in Figure 6.3(a) and its equivalent circuit representation is shown in Figure 6.3(b). The normalised susceptance obtained is plotted against normalised frequency in Figure 6.4.

The waveguide stub was modeled using approximately 100 equally-spaced nodes. Very good agreement with theoretical values for susceptance was obtained. However, since no higher-mode fields are produced, due to the symmetry of the problem, there is no advantage in using the projective-port method over the Dirichlet-port method.

6.6 - The Inductive Window

The inductive window, depicted in Figure 6.5(a), provides a good test of the effectiveness of the projective-port method over the Dirichlet-port method. The equivalent circuit parameters for this two-port are shown in Figure 6.5(b).

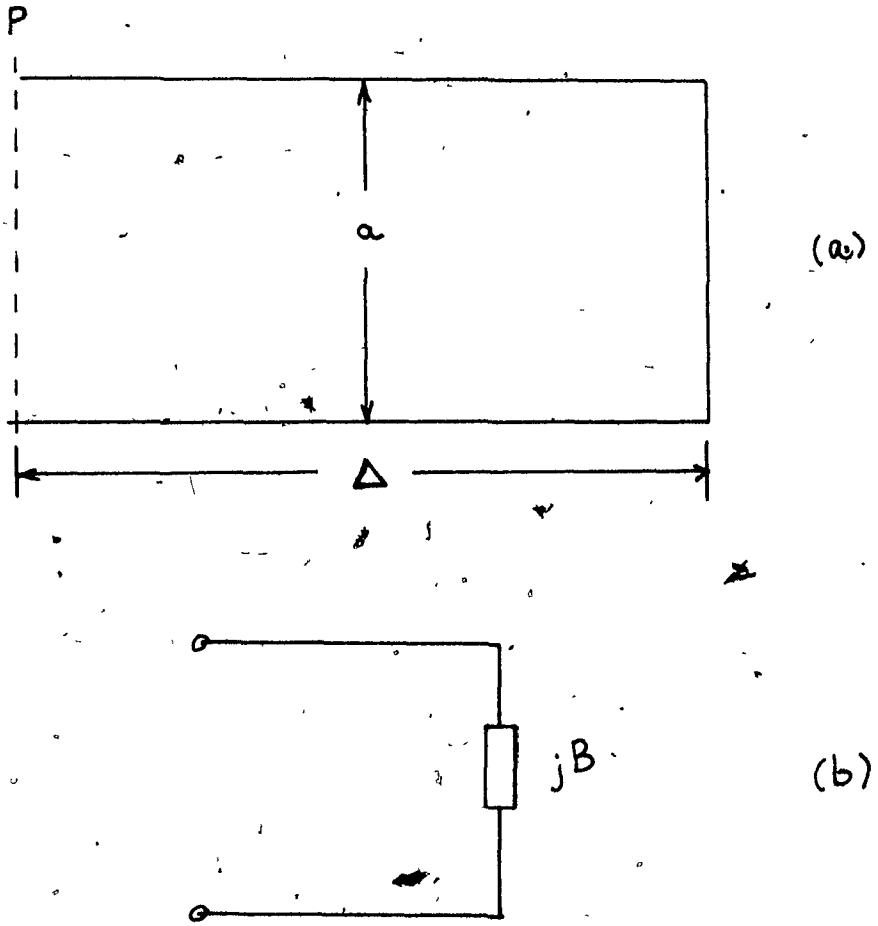

FIG 6.3 THE EMPTY RECTANGULAR WAVEGUIDE

(a) H-plane view
(b) Equivalent circuit

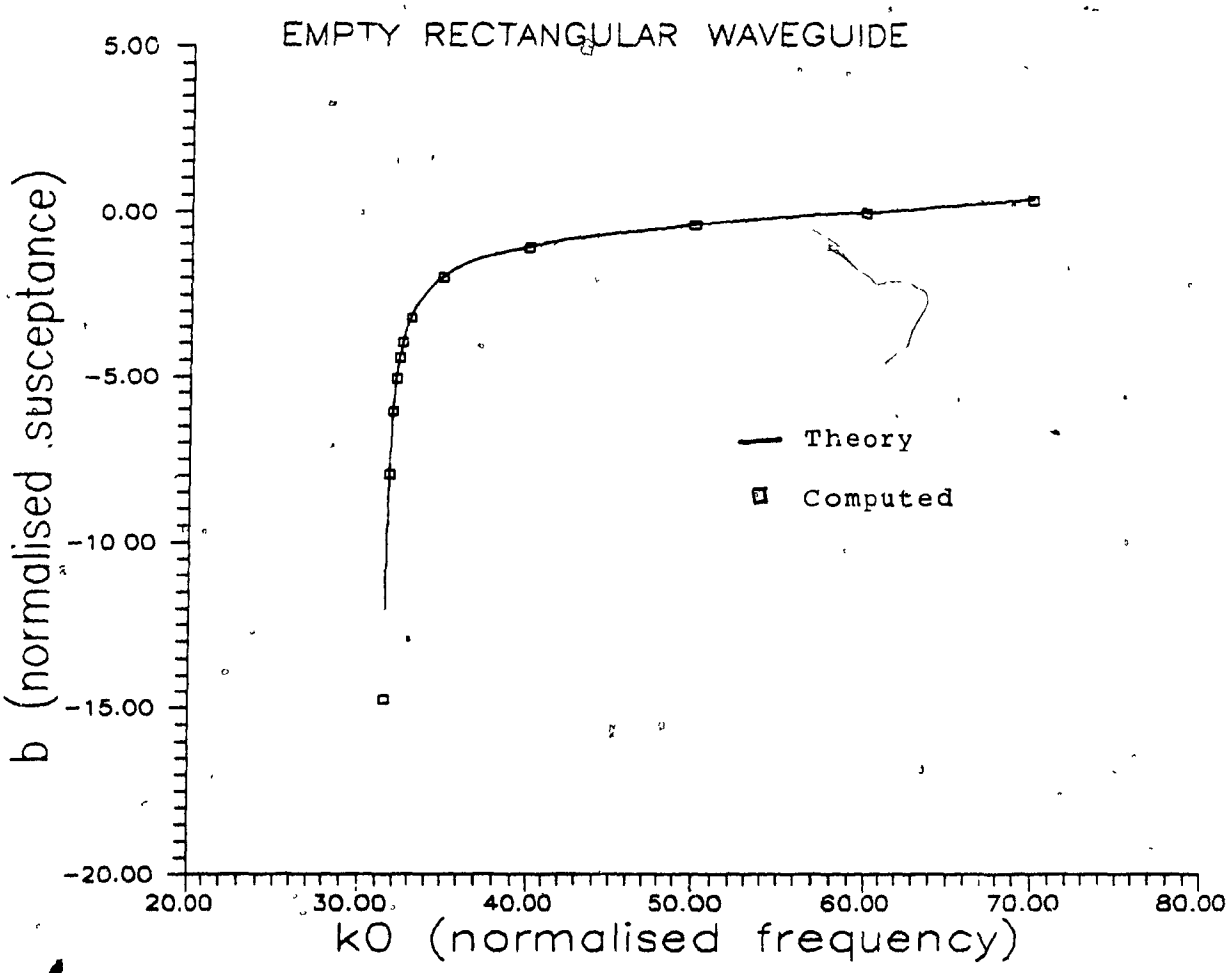

FIG 6.4 THE EMPTY WAVEGUIDE

(B vs. Frequency)

A plot of the reactances, X_a and X_b, is given in Figures 6.6 and 6.7 for parameter values $d' = 0.6m.$, $a = 1.0m.$, and $l = 0.2m.$ in Figure 6.5(a). Results from the projective-port and Dirichlet-port methods are compared with the values predicted by Marcuvitz[5]. The port plane was defined to be 0.3 m. away from the terminal plane, T, of the junction. The finite element model consisted of approximately 200 nodes, with more refinement near the obstacles.

The projective-port method results correspond more closely to the Marcuvitz results than do the Dirichlet-port results. The reason for this is that the Dirichlet-port method does not account for the higher-mode contributions at the port plane, which are significant for this problem. As a result, the projective-port method gives better results with the same discretisation.

The results obtained for this test problem differ significantly from the Marcuvitz results, however. The reason for this may be that the sharp edges of the inductive window produce large variations in the y-component of electric field, locally. As a result, many more degrees of freedom are needed to model the inductive window accurately. However, an even higher number of nodes are required for the Dirichlet-port method than for the projective-port method.

6.7 - The Circular Metallic Post

Another test example which generates a significant higher-mode field contribution is that of the circular metallic obstacle in a waveguide, shown in Figure 6.8(a), with $a = 1.0m.$, d/a ranging from 0.05 to 0.25, and $\lambda/a = 1.4$. The equivalent circuit representation of this two-port is shown in Figure 6.8(b). This junction was modeled using approximately 400 finite element nodes.

The parameters X_a and X_b are plotted versus post diameter in Figures 6.9

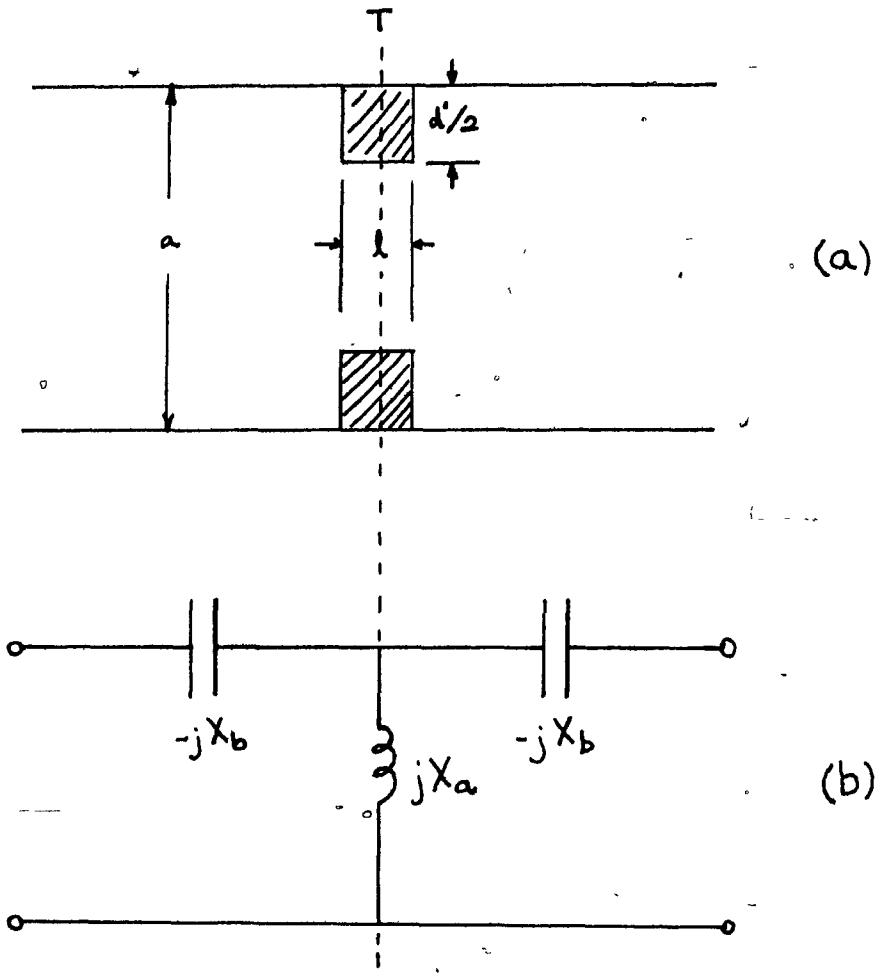

FIG 6.5 THE INDUCTIVE WINDOW

(a) H-plane view
(b) Equivalent circuit

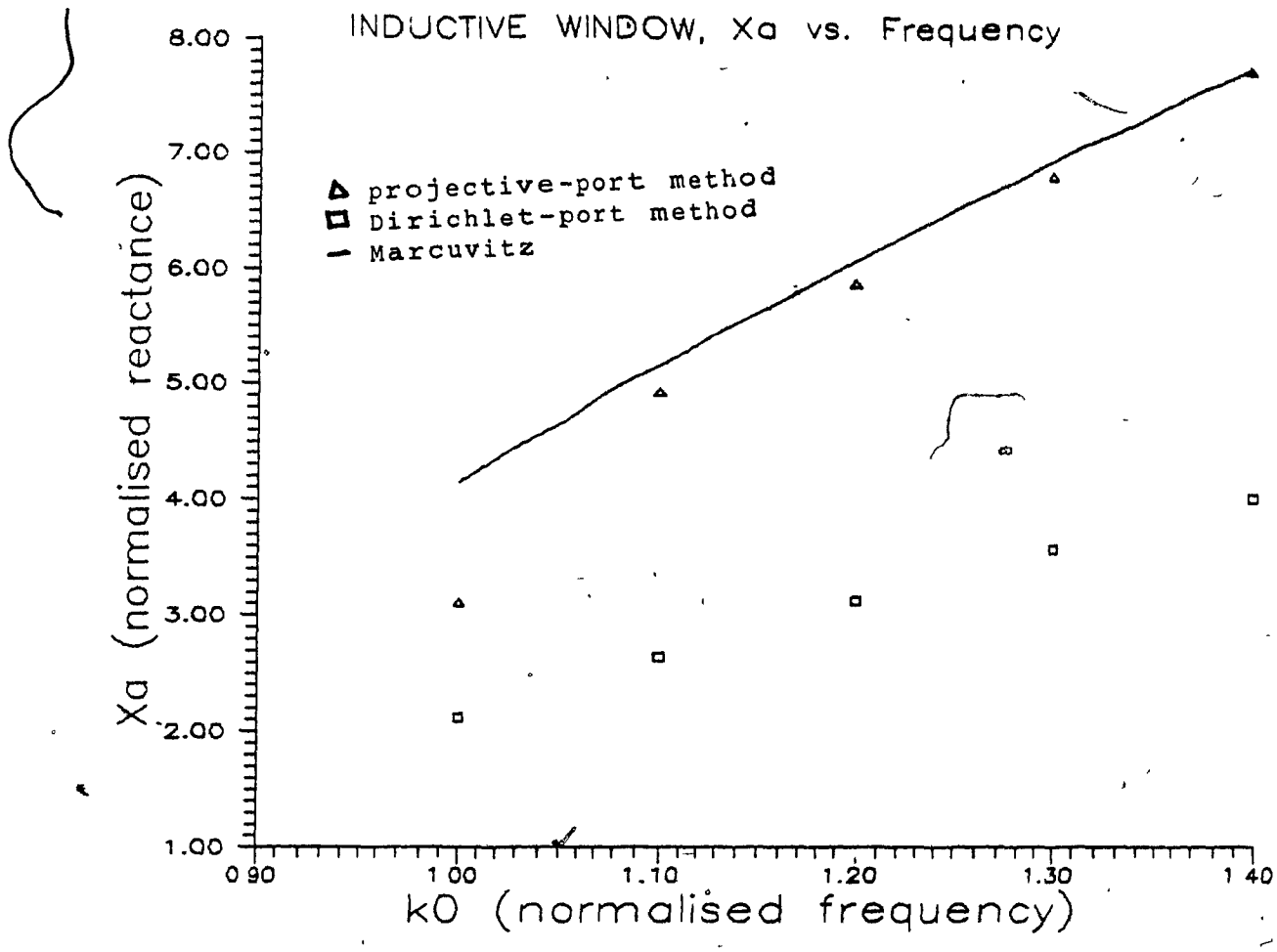

FIG 6.6 THE INDUCTIVE WINDOW

(X_a vs. Frequency)

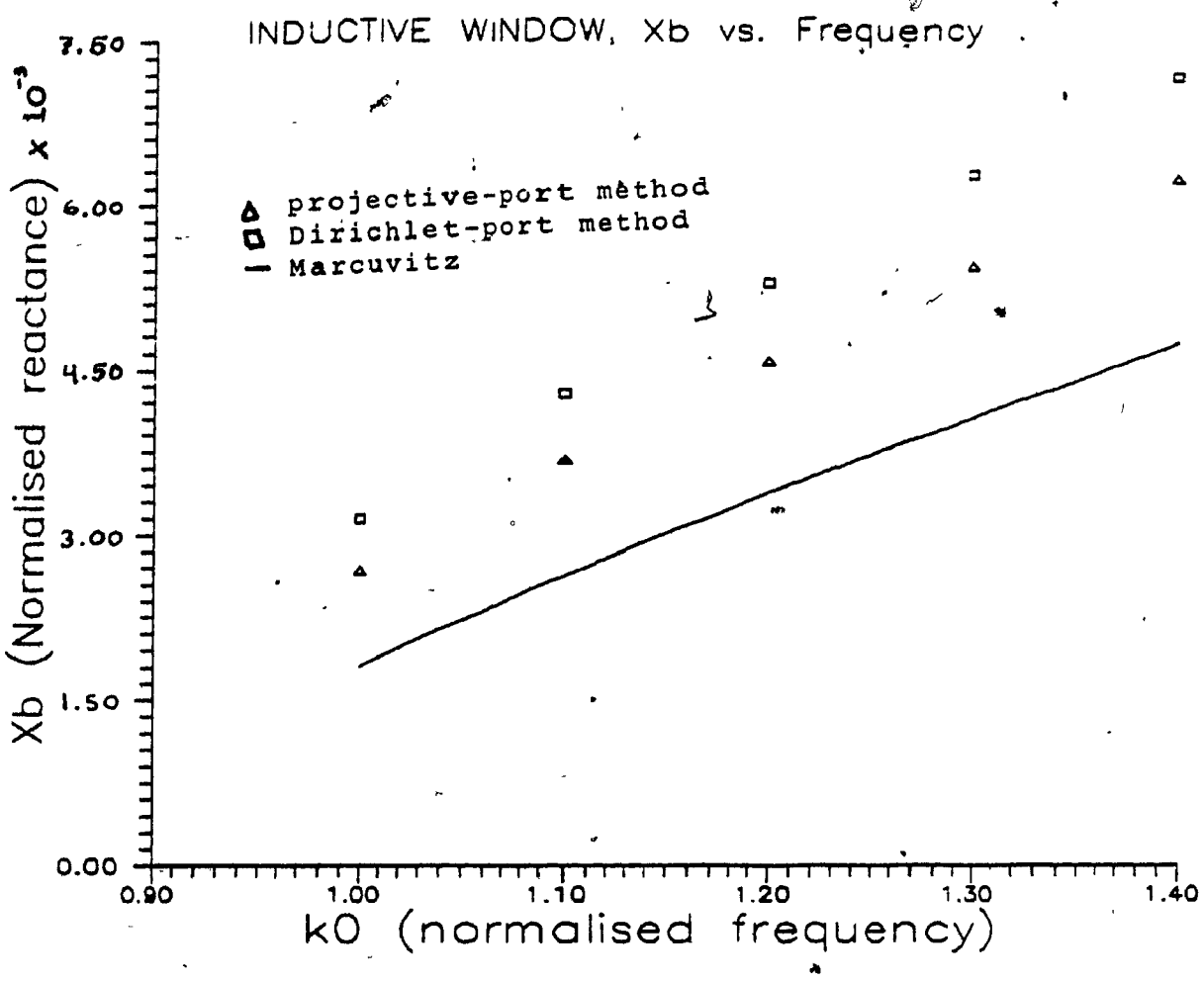

FIG 6.7 THE INDUCTIVE WINDOW

(X_b vs. Frequency)

and 6.10. Again, the two finite element methods are

compared with the predicted values from Marcuvitz[5] in both of these graphs.

It is interesting to note that due to the close placement of the port plane (0.2 m.) the projective-port results correspond more closely to Marcuvitz[5] results than do the Dirichlet-port results. In addition, this effect becomes more pronounced as the post diameter is increased. Presumably, this corresponds to an increasing higher-mode field contribution at the port plane.

6.8 - Summary

This chapter presents a finite element formulation, based upon the theory of Chapter 5, which extracts network parameters for one- and two-port H-plane waveguide junctions. The results obtained from a FORTRAN program indicate that the projective-port method, introduced in this thesis, models certain junctions better than does the standard Dirichlet-port method [1]. In particular, the projective-port method is particularly well suited to problems in which the port plane has been defined close enough to the junction that higher-mode fields are significant. This is evident in two test examples presented in this chapter: the inductive window; and the circular metallic post obstacle.

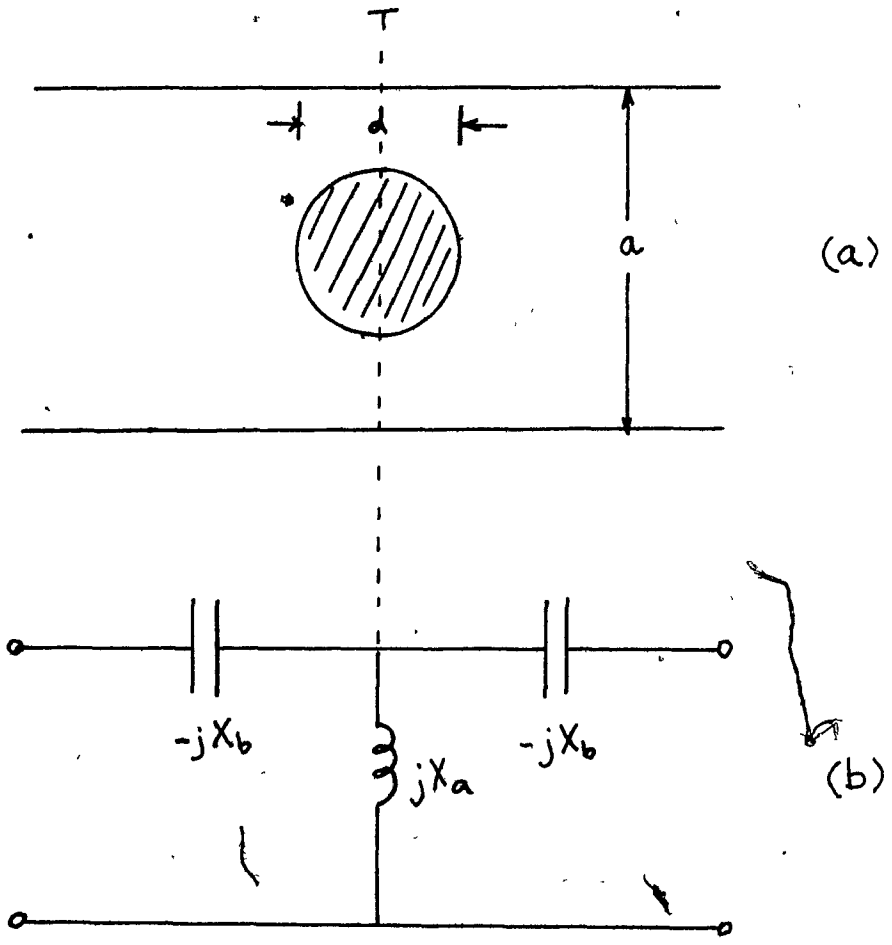

FIG 6.8 THE CIRCULAR METALLIC POST

(a) H-plane view
(b) Equivalent circuit

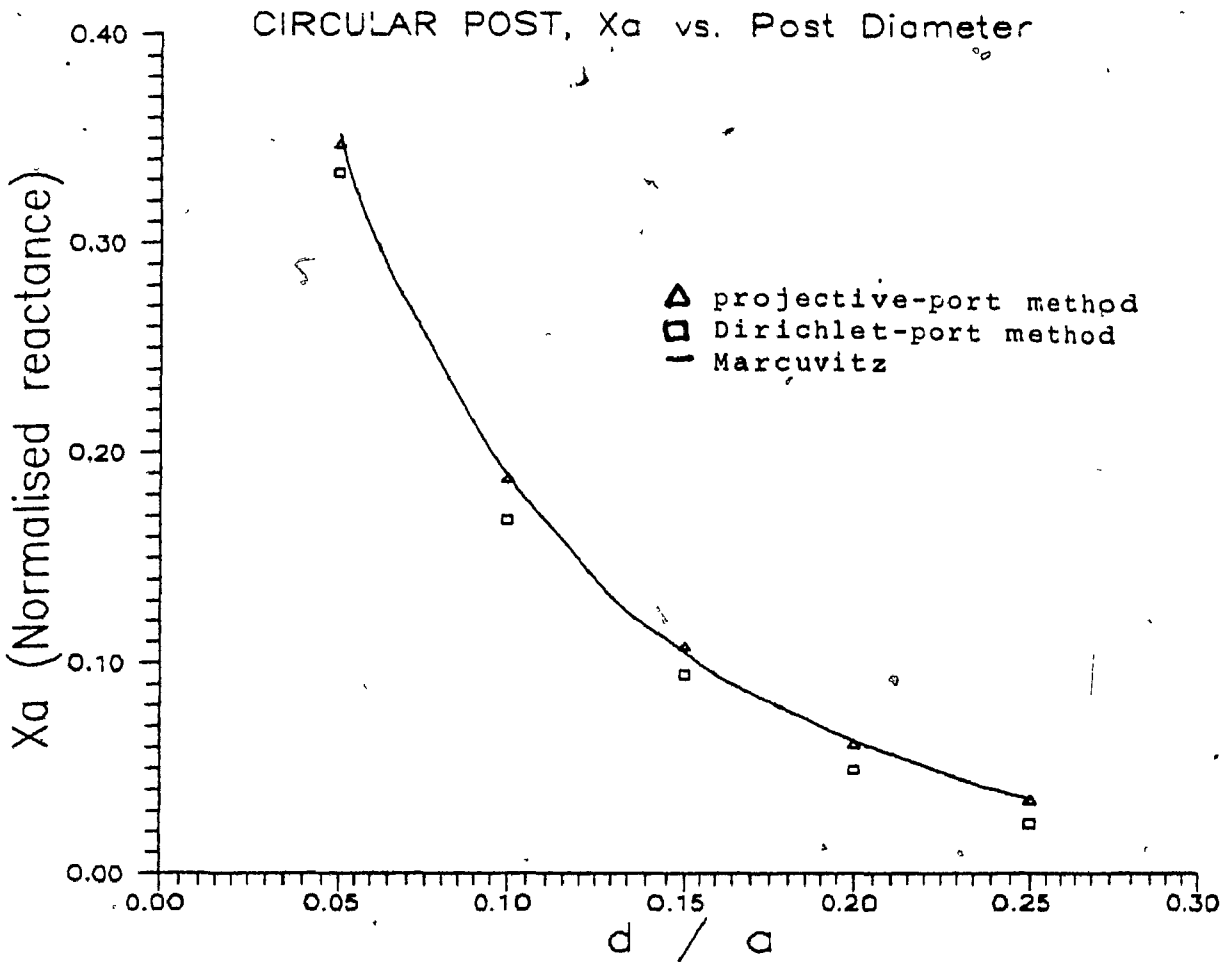

FIG 6.9 THE CIRCULAR METALLIC POST

(X_a vs. Post diameter)

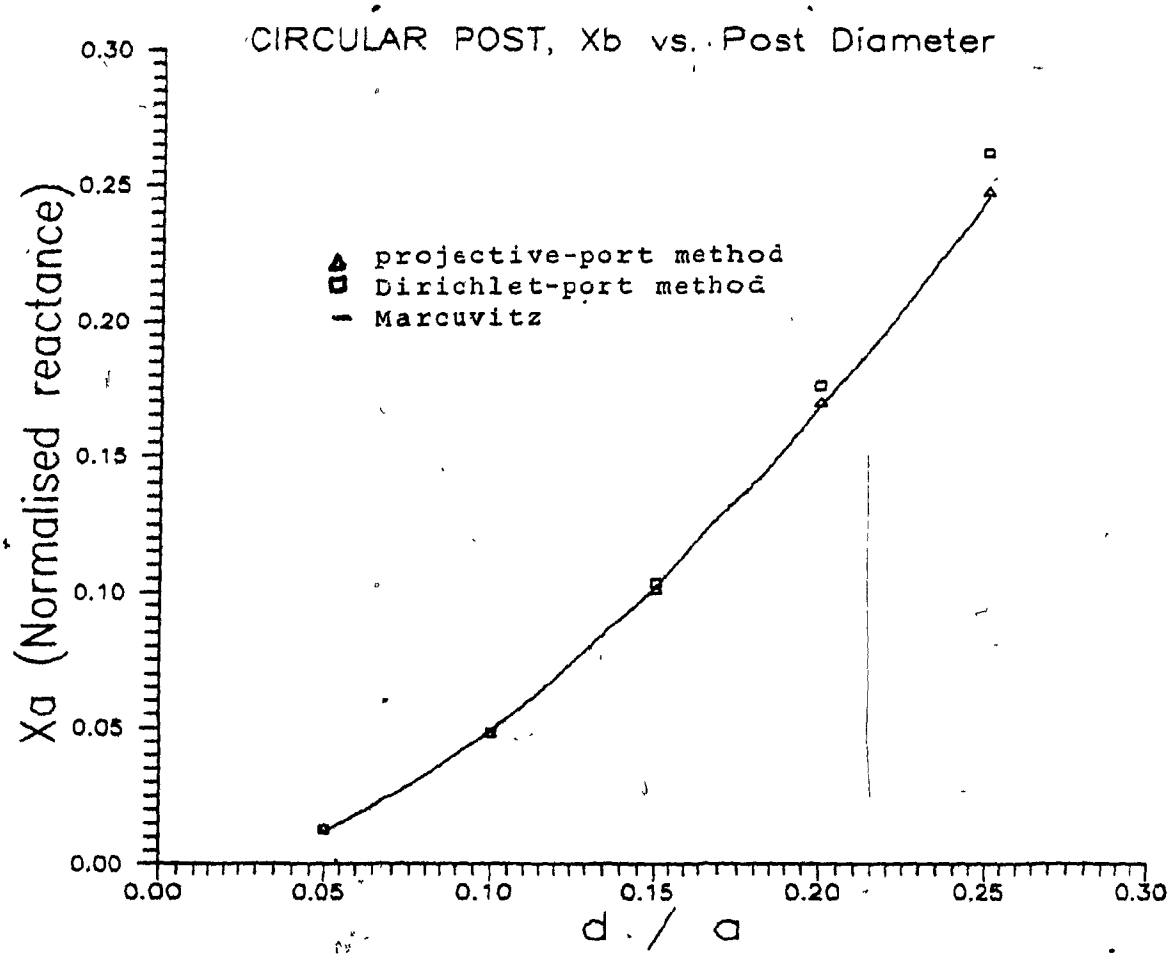

FIG 6.10 THE CIRCULAR METALLIC POST

(X_b vs. Post diameter)

Chapter 7 - Conclusion

The design of passive microwave components requires the use of flexible, reliable computational tools. Useful tools of this type can provide the microwave engineer with a circuit parameter representation for a given waveguide device. Several formulations currently exist which are able to characterise H-plane waveguide junctions in terms of admittance or impedance matrix representations [1][2][3][4]. However, the current methods have some restrictions regarding the placement of the port planes. This thesis has presented a finite element method to obtain admittance parameters of H-plane waveguide junctions, which is free of port placement restrictions.

Previous methods to extract network parameters of H-plane waveguide junctions have been presented by Webb [1] and Koshiba [2][3][4]. The Dirichlet-port method, used by Webb, is a finite element, scalar, electric-field formulation. The method does not, however, account for evanescent modes in the waveguides connected to the junction. As a result, the junction ports must be placed a large distance away from the junction cavity so that only the dominant-mode fields exist there. In using the Dirichlet-port method, a microwave designer must therefore have some *a priori* knowledge of the field distribution in the junction. This presents an inconvenience to the designer.

The Koshiba methods are scalar [2][4][25] and vector [3] electric and magnetic field which account for the evanescent modes between two ports planes, thereby allowing the ports to be defined arbitrariy close to the junction. However, for each port, two planes must be defined with a significant number of finite element nodes in the region between them. This structure is inconvenient, although it is an improvement on the Dirichlet-port method. Furthermore, the number of nodes in the region between the two port planes may increase the number of degrees of freedom needed to solve the problem. In addition, the resulting finite element matrix is not symmetric, thus requiring longer solution times than for symmetric or positive definite matrices.

The method presented in this thesis is similar to the method used by Webb [1] but makes use of modal projection operators to account for evanescent modes in the waveguides connected to the ports of the junction. Only one port plane is required for each port, and accordingly, fewer degrees of freedom are required to solve the waveguide problem, thereby making the method more amenable to fast computation than Koshiba's method. Furthermore, the symmetry of the matrix operator is preserved, leading to still faster solution times.

The functional used in the new method can also be shown to be positive definite for a portion of the driving frequency spectrum. The resulting matrix equation may therefore be solved using the conjugate-gradient method, leading to lower solution times. Also, when the matrix is positive definite, the one-port admittance parameters found by this method are lower bounds for the true admittances.

Numerical results, obtained from a Fortran implementation of the new method, correspond well with theoretical network parameters found in Marcuvitz [5].

Test examples used in this thesis include an empty, short-circuited waveguide, an inductive window in a rectangular guide, and a circular metallic post in a rectangular guide. The results of this method were compared to results obtained from the method in Webb [1] and were shown to outperform the latter for waveguide junctions having significant higher-mode contributions at the port planes.

Improvements or extensions to the new method could be pursued along several fronts. Firstly, the accuracy of computed parameters could be increased by using higher order finite elements. However, substantial work would be required to convert the modal operators for higher order elements. Another extension would be to investigate dual bounding methods (see Synge's hypercircle method [28]) to obtain tight bounds on the network parameters, in order to estimate the error of a given admittance parameter. As is, the method only yields lower bounds on the admittance parameters, making it impossible to extract a measure of the accuracy of the computed parameters.

As a final extension, a vector electric or magnetic field formulation could provide an alternate approach to the problem of waveguide analysis, thereby allowing a broader class of waveguide junction to be analysed. In fact, the modal approach to waveguide problems could be applied to a junction of any waveguide - indeed, the mathematics has been presented for a general, three-dimensional junction problem.

Appendix I - The Physical Significance of $F_0(\tilde{E})$

The functional $F_0(\tilde{E})$, evaluated at its stationary point, $\tilde{E}$, can be related to the admittance seen at a given port. (Refer to Figure 4.1 for problem geometry). The functional at $\tilde{E}$ is:

$$F_0(\underline{\tilde{E}}) = \int_\Omega \left\{ \frac{1}{\mu_r} (\underline{\nabla} \times \underline{\tilde{E}})^2 - k_0^2 \epsilon_r \underline{\tilde{E}} \cdot \underline{\tilde{E}} \right\} d\Omega \qquad (A1.1)$$

Since $\underline{\nabla} \cdot (\underline{a} \times \underline{b}) = \underline{b} \cdot (\underline{\nabla} \times \underline{a}) - \underline{a} \cdot (\underline{\nabla} \times \underline{b})$, if the substitution $\underline{b} = \underline{\nabla} \times \underline{a}$ is made, the functional may be written:

$$F_0(\underline{\tilde{E}}) = \int_\Omega \left\{ \underline{\nabla} \cdot (\underline{\tilde{E}} \times \underline{\nabla} \times \underline{\tilde{E}}) + \underline{\tilde{E}} \cdot (\underline{\nabla} \times \underline{\nabla} \times \underline{\tilde{E}}) - k_0^2 \epsilon_r \underline{\tilde{E}} \cdot \underline{\tilde{E}} \right\} d\Omega \qquad (A1.2)$$

And by the Divergence Theorem:

$$F_0(\underline{\tilde{E}}) = \int_{\partial\Omega} \frac{1}{\mu_r} \underline{\tilde{E}} \times \underline{\nabla} \times \underline{\tilde{E}} \cdot \underline{n} \, dS + \int_\Omega \underline{\tilde{E}} \cdot (\underline{\nabla} \times \underline{\nabla} \times \underline{\tilde{E}} - k_0^2 \epsilon_r \underline{\tilde{E}}) \, d\Omega \qquad (A1.3)$$

Using Maxwell's first equation ((3.1)a),

$$F_0(\underline{\tilde{E}}) = j\omega \int_{\partial\Omega} \underline{\tilde{E}} \times \underline{\tilde{H}} \cdot \underline{n} \, dS + \int_\Omega \underline{\tilde{E}} \cdot (\underline{\nabla} \times \underline{\nabla} \times \underline{\tilde{E}} - k_0^2 \epsilon_r \underline{\tilde{E}}) \, d\Omega \qquad (A1.4)$$

Since $\tilde{E}$ satisfies the curl-curl equation, the second term vanishes so that:

$$F_0(\underline{\tilde{E}}) = j\omega \int_{\partial\Omega} \underline{\tilde{E}} \times \underline{\tilde{H}} \cdot \underline{n} \, dS \qquad (A1.5)$$

Therefore, $F_0(\tilde{E})$ is proportional to the average outward-going reactive power leaving the junction. However, due to the conducting walls of the junction, power leaves

or enters only from the port surface, $\partial\Omega_p$:

$$F_0(\underline{\tilde{E}}) = j\omega \int_{\partial\Omega_p} \underline{\tilde{E}} \times \underline{\tilde{H}} \cdot \underline{n}\, dS \qquad (A1.6)$$

If the port is far enough away from the junction cavity, only the dominant-mode fields are present at $\partial\Omega_p$. If the port is then excited with a unit-voltage ($V_1 = 1$) wave:

$$\begin{aligned} \underline{\tilde{E}} &= \underline{e}_1 \quad \text{at } \partial\Omega_p \\ \underline{\tilde{H}} &= I_1 \underline{h}_1 \quad \text{at } \partial\Omega_p \end{aligned} \qquad (A1.6b)$$

And the functional reduces to:

$$F_0(\underline{\tilde{E}}) = j\omega I_1 \int_{\partial\Omega_p} \underline{e}_1 \times \underline{h}_1 \cdot \underline{n}\, dS \qquad (A1.7)$$

Since the amplitudes of $\underline{e}_1$ and $\underline{h}_1$ are arbitrary, the functional is:

$$F_0(\underline{\tilde{E}}) = K \cdot I_1 \qquad (A1.8)$$

where K is a number which depends upon ω and the amplitudes of $\underline{e}_1$ and $\underline{h}_1$.

Now I_1 is the admittance when a unit voltage wave is applied, therefore:

$$F_0(\underline{\tilde{E}}) = K \cdot y \qquad (A1.9)$$

Appendix II - Some Functional Analysis Theory

This appendix will restate the H-plane junction boundary problem of Chapters 3,4 and 5 in a more mathematically-rigorous form. An investigation of the positive definite properties of operators will follow.

A2.1 - The Boundary Value Problem

The H-plane waveguide problem can be formulated as a scalar field problem, involving only the y-component of electric field. In this case, the curl-curl functional for $u = E_y$ reduces to :

$$F_0(u) = \int_\Omega \left\{ \frac{1}{\mu_r} (\nabla u)^2 - k_0^2 \epsilon_r u^2 \right\} \, d\Omega \qquad (A2.1)$$

and is subject to :

$$u = 0 \quad \text{on } \partial\Omega_c \text{ (conductor).}$$

$$P(u) = g \quad \text{on } \partial\Omega_p \text{ (port boundary).}$$

The functional represents a quadratic form, which may be written as :

$$F_0(u) = \langle \mathcal{L}u, u \rangle - k_0^2 \langle \epsilon_r u, u \rangle \qquad (A2.2)$$

$$\text{where} \quad \langle \mathcal{L}u, u \rangle = \int_\Omega \frac{1}{\mu_r} |\nabla u|^2 \, d\Omega$$

$$\langle \epsilon_r u, u \rangle = \int_\Omega \epsilon_r u^2 \, d\Omega$$

A quadratic form may be one of the three types depicted in Figure A2.1. If $\tilde{u}$ is the stationary point of $F(u)$ and $F(u)$ is positive definite (i.e. $F(u) > 0 \quad \forall u \neq 0$), then :

$$F(u) \geq F(\tilde{u}) = \tilde{f} \tag{A2.3}$$

and $F(u)$ is said to bound the quantity $\tilde{f}$. An operator, $\mathcal{L}$, whose quadratic form, $< \mathcal{L}u, u >$, is positive definite, is called a positive definite operator.

A2.2 - Correspondence Between the Eigen Problem and the Driven Problem

The eigen problem associated with a given operator, $\mathcal{L}$, consists of determining all λ_i and $u_i \neq 0$, such that :

$$\mathcal{L}u_i - \lambda_i u_i = 0 \qquad i = 1, 2, \ldots \tag{A2.4}$$

$$u_i = 0 \quad \text{on } \partial\Omega_u$$

$$P(u_i) = 0 \quad \text{on } \partial\Omega_p$$

If all λ_i are real and positive, then the $\mathcal{L}$ is positive definite.

The driven problem involves finding a $\tilde{u}$ such that :

$$\mathcal{L}\tilde{u} - \lambda_0 \tilde{u} = 0 \tag{A2.5}$$

$$\tilde{u} = 0 \quad \text{on } \partial\Omega_u$$

$$P(\tilde{u}) = g \quad \text{on } \partial\Omega_p$$

Equation (A2.5) may be restated in the simpler form :

$$\mathcal{L}'u = 0 \tag{A2.6}$$

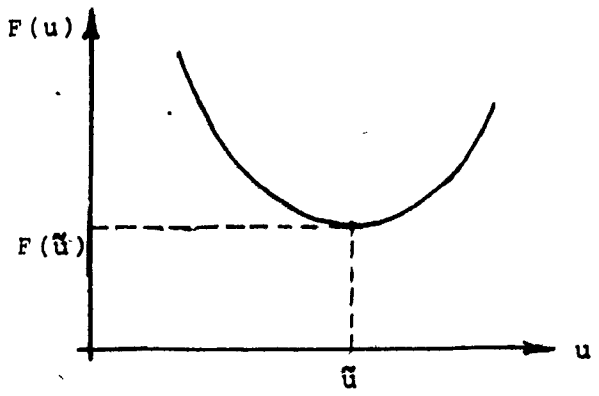

positive definite

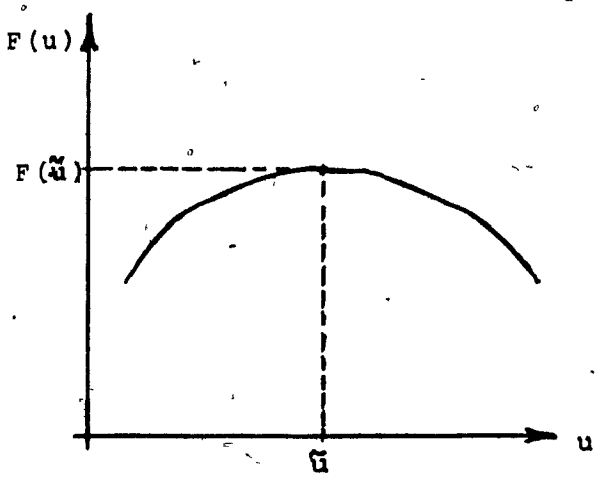

negative definite

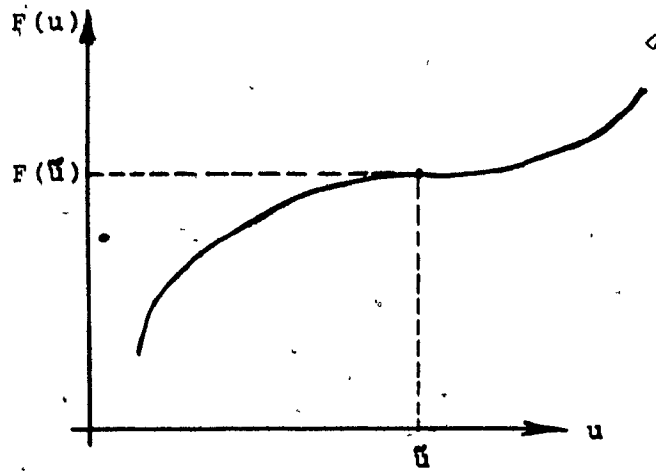

indefinite

FIG A2.1 THREE TYPES OF OPERATORS

where $\mathcal{L}' = \mathcal{L} - \lambda_0 \mathbf{I}$

and $\mathbf{I}$ is the identity operator.

The operator $\mathcal{L}'$ is positive definite, in turn, if all of its eigenvalues, $\lambda_{,,}$, are real and positive. If the $\lambda_{,}$ and $\lambda_{,,}$ are numbered from lowest to highest, such that :

$$\begin{aligned} &\lambda_1 \leq \lambda_2 \leq \lambda_3 \leq \cdots \leq \lambda_n \\ &\lambda'_1 \leq \lambda'_2 \leq \lambda'_3 \leq \cdots \leq \lambda'_n \end{aligned} \qquad (A2.6b)$$

then $\lambda_{,,}$ may be expressed as :

$$\lambda'_i = \lambda_i - \lambda_0 \qquad (A2.7)$$

The smallest eigenvalue of $\mathcal{L}'$ is therefore :

$$\lambda'_1 = \lambda_1 - \lambda_0 \qquad (A2.8)$$

Equation (A2.8) provides a condition on the positive definiteness of $\mathcal{L}'$:

Theorem 1: The operator $\mathcal{L}'$ is positive definite if:

$(i)\mathcal{L}$ is positive definite $(\lambda_1 > 0)$

$(ii)\lambda_0 < \lambda_1 =$ smallest eigenvalue of $\mathcal{L}$

A2.3 - Addition of Semi-Definite Operators to $\mathcal{L}'$

The operator, $\mathcal{L}'$ remains positive definite upon addition of a positive semi-definite operator, **A**.

Theorem 2: The operator $\mathbf{M} = \mathcal{L}' + \mathbf{A}$ if:

$(i)\mathcal{L}$ is positive definite

$(ii)\mathbf{A}$ is positive semi-definite

Proof: $\langle \mathbf{A}u, u \rangle \geq 0$ by definition, therefore:

$$F(u) = \langle \mathbf{M}u, u \rangle \geq \langle \mathcal{L}'u, u \rangle > 0 \; \forall \; u \neq 0$$

Therefore $\mathbf{M}$ is positive definite.

A2.4 - The Positive Definiteness of $F(u)$

Theorem 1 may be applied to the functional of equation (A2.1), so that $F_0(u)$ is positive definite if $k_0^2 \epsilon_r < \lambda_1$, where λ_1 corresponds to the first cavity resonant frequency of the junction problem. In addition, the functional presented in Chapter 5 may be analysed using Theorem 2. First, note that $F(u)$ can be expressed as (see Appendix III) :

$$F(u) = F_0(u) + \sum_{m=2}^{\infty} T_m \left(\int_{\partial\Omega_p} u \sin \frac{m\pi x}{a} \, dx \right)^2 \qquad (A2.9)$$

where T_m is a positive scalar function of m. The second (boundary) term in equation (A2.9) is a positive semi-definite quadratic form, by inspection. Theorem 2 may be applied to equation (A2.9) with the result : $F(u)$ is positive definite if $k_0^2 \epsilon_r < \lambda_1$. This statement demonstrates that if the driving waveguide frequency is low enough, then $F(u)$ is positive definite.

Appendix III - The Boundary Term in $F(\underline{E})$

The boundary term in $F(\underline{E})$ presented in Chapter 5 may be assembled by assuming the finite element nodes along the port boundary are part of a large "port-element". If the port nodes in Figure 6.1(a) are assumed to be equally-spaced along $\partial\Omega$, then the boundary term simplifies to:

$$F(\underline{E}) - F_0(\underline{E}) = jk_0\eta_0 \sum_{m=2}^{\infty} y_m \int_{x'=0}^{x'=a} \left[E_y \underline{a}_y \cdot \left\{ \frac{\int_{\partial\Omega_p} E_y \underline{a}_y \cdot \underline{e}_m \, d\Omega_p}{\int_{\partial\Omega_p} \underline{e}_m \cdot \underline{e}_m \, d\Omega_p} \right\} \cdot \underline{e}_m \right] dx'$$

$$= jk_0\eta_0 \sum_{m=2}^{\infty} y_m \cdot \frac{2}{a} \cdot \left[\int_{x'=0}^{x'=a} E_y \sin \tfrac{m\pi x'}{a} \, dx' \right]^2$$

$$= \frac{2jk_0\eta_0}{a} \sum_{m=2}^{\infty} y_m \left[\int_{x'=0}^{x'=a} E_y \sin \tfrac{m\pi x'}{a} \, dx' \right]^2$$

Now $E_y = \sum_{i=1}^{n_0} E_i \alpha_i$ where E_i are nodal E_y-values along the port and α_i are global α-polynomial functions (see Figure 6.1(b)). The boundary term is therefore:

$$B.T. = \sum_{m=2}^{\infty} R_m \left[\int_{x'=0}^{x'=a} \sum_{i=1}^{n_0} E_i \alpha_i \sin \tfrac{m\pi x'}{a} \, dx' \right]^2$$

$$= \sum_{m=2}^{\infty} R_m \sum_{i=1}^{n_0} \sum_{j=1}^{n_0} E_i E_j \int_{x'=0}^{x'=a} \alpha_i \sin \tfrac{m\pi x'}{a} \, dx' \cdot \int_{x''=0}^{x''=a} \alpha_j \sin \tfrac{m\pi x''}{a} \, dx''$$

$$= \sum_{m=2}^{\infty} R_m \sum_{i=1}^{n_0} \sum_{j=1}^{n_0} E_i E_j K_i^m \cdot K_j^m$$

where

$$K_i^m = \int_{x'=0}^{x'=a} \alpha_i \sin \tfrac{m\pi x'}{a}\, dx'$$

$$R_m = \frac{2jk_0\eta_0 y_m}{a}$$

Now for arbitrary i, K_i^m has the form:

$$K_i^m = \int_{x_i-\omega}^{x_i} \left(1 + \frac{x' - x_i}{\omega}\right) \sin \tfrac{m\pi x'}{a}\, dx' + \int_{x_i}^{x_i+\omega} \left(1 - \frac{x' - x_i}{\omega}\right) \sin \tfrac{m\pi x'}{a}\, dx'$$

$$= \int_{x_i-\omega}^{x_i} \sin \tfrac{m\pi x'}{a}\, dx' + \frac{1}{\omega}\int_{x_i-\omega}^{x_i} x' \sin \tfrac{m\pi x'}{a}\, dx' - \frac{1}{\omega}\int_{x_i-\omega}^{x_i} x_i \sin \tfrac{m\pi x'}{a}\, dx'$$

$$+ \int_{x_i}^{x_i+\omega} \sin \tfrac{m\pi x'}{a}\, dx' - \frac{1}{\omega}\int_{x_i}^{x_i+\omega} x' \sin \tfrac{m\pi x'}{a}\, dx' + \frac{1}{\omega}\int_{x_i}^{x_i+\omega} x_i \sin \tfrac{m\pi x'}{a}\, dx'$$

$$= \left[-\frac{a}{m\pi}\cos \tfrac{m\pi x'}{a}\right]_{x_i-\omega}^{x_i} + \frac{1}{\omega}\left[\frac{a^2}{m^2\pi^2}\sin \tfrac{m\pi x'}{a} - \frac{a}{m\pi}x' \cos \tfrac{m\pi x'}{a}\right]_{x_i-\omega}^{x_i}$$

$$- \frac{1}{\omega}\left[-\frac{a}{m\pi}x_i \cos \tfrac{m\pi x'}{a}\right]_{x_i-\omega}^{x_i} + \left[-\frac{a}{m\pi}\cos \tfrac{m\pi x'}{a}\right]_{x_i}^{x_i+\omega}$$

$$- \frac{1}{\omega}\left[\frac{a^2}{m^2\pi^2}\sin \tfrac{m\pi x'}{a} - \frac{a}{m\pi}x' \cos \tfrac{m\pi x'}{a}\right]_{x_i}^{x_i+\omega} + \frac{1}{\omega}\left[-\frac{a}{m\pi}x_i \cos \tfrac{m\pi x'}{a}\right]_{x_i}^{x_i+\omega}$$

Let

$$w \equiv \text{port node spacing}$$

$$x_i^- \equiv x_i - \omega$$

$$x_i^+ \equiv x_i + \omega$$

therefore,

$$K_i^m = \frac{a^2}{\omega m^2\pi^2}\left\{2\sin\frac{m\pi x_i}{a} - \sin\frac{m\pi x_i^-}{a} - \sin\frac{m\pi x_i^+}{a}\right\}$$

Going back to the original expression for F:

$$F(\underline{E}) = F_0(\underline{E}) + \frac{2jk_0\eta_0}{a} \sum_{m=2}^{\infty} y_m \sum_{i=1}^{n0} \sum_{j=1}^{n0} E_i E_j \frac{a^4}{\omega^2 m^4 \pi^4} \{\eta_i\}\{\eta_j\}$$

with

$$y_m = \frac{|\sqrt{\frac{m^2\pi^2}{a^2} - k_0^2}|}{jk_0\eta_0}$$

$$\eta_i = \left\{2sin\frac{m\pi x_i}{a} - sin\frac{m\pi x_i^-}{a} - sin\frac{m\pi x_i^+}{a}\right\}$$

$$\eta_j = \left\{2sin\frac{m\pi x_j}{a} - sin\frac{m\pi x_j^-}{a} - sin\frac{m\pi x_j^+}{a}\right\}$$

so that $F(\underline{E})$ takes the form:

$$F(\underline{E}) = F_0(\underline{E}) + \frac{2a^3}{\omega^2\pi^4} \sum_{m=2}^{\infty} \frac{|\sqrt{\frac{m^2\pi^2}{a^2} - k_0^2}|}{m^4} \sum_{i=1}^{n0} \sum_{j=1}^{n0} E_i E_j \{\eta_i\}\{\eta_j\},$$

which is positive semi-definite and converges.

REFERENCES

1. Webb, J.P., and Parihar, S., "Finite element analysis of H-plane waveguide problems," *IEE Proc.*, vol. 133(H), no. 2, 1986, pp. 91–94.

2. Koshiba, M., and Suzuki, M., "Finite element analysis of H-plane waveguide junction with arbitrarily shaped ferrite post," *IEEE Trans. Microw. Theor. Techn.*, vol. MTT-34, 1986, pp. 103–109.

3. Koshiba, M., Sato, M., and Suzuki, M., "Application of the finite element method to H-plane waveguide discontinuities," *Elec. Lett.*, vol. 18, no. 9, 1982, pp. 364–365.

4. Koshiba, M., Sato, M., and Suzuki, M., "Finite element analysis of arbitrarily shaped H-plane waveguide discontinuities," *Trans. IECE Japan*, vol. E66, no. 2, 1983, pp. 82–87.

5. Marcuvitz, N., *Waveguide handbook*, McGraw-Hill, New York, 1951.

6. Matsumaru, K., "Reflection coefficient of E-plane tapered waveguides," *IRE Trans. Microw. Theor. Techn.*, vol. MTT-6, 1958, pp. 143–149.

7. Collin, R.E., *Foundations of microwave engineering*, McGraw-Hill, New York, 1966.

8. Southwell, R.V., *Relaxation methods in theoretical physics*, Oxford Press, Oxford, 1946.

9. Grad, E.M., "Solution of electrical engineering problems by Southwell's relaxation method," *Trans. AIEE*, vol. 71, no. 1, 1952, pp. 205–214.

10. Davies, J.B., and Cohen, P., "Theoretical design of symmetrical junction stripline circulators," *IEEE Trans. Microw. Theor. Techn.*, vol. MTT-11, 1963, pp. 506–512.

11. Davies, J.B., "An analysis of the m-port symmetrical H-plane waveguide junction with central ferrite post," *IEEE Trans. Microw. Theor. Techn.*, vol. MTT-10, 1962, pp. 596–604.

12. Green, H.E., "The numerical solution of some important transmission line problems," *IEEE Trans. Microw. Theor. Techn.*, vol. MTT-13, 1965, pp. 676–692.

13. Schneider, M.V., "Computation of impedance and attenuation of TEM liness by finite difference methods," *IEEE Transs. Microw. Theor. Techn.*, vol. MTT-13, no. 6, 1965, pp. 793–800.

14. Metcalfe, W.S., "Characteristic impedance of retangular transmission lines," *Proc. IEE*, vol. 112, no. 11, 1965, pp. 2033–2039.

15. Carson, C.T., "The numerical solution of TEM mode transmission lines with curved boundaries," *IEEE Trans. Microw. Theor. Techn.*, vol. MTT-15, 1967, pp. 269–270.

16. Muilwyk, C.A., and Davies, J.B., "The numerical solution of rectangular waveguide junctions and discontinuities of arbitrary cross-section," *IEEE Trans. Microw. Theor. Techn.*, vol. MTT-15, 1967, pp. 450–455.

17. Wexler, A., "Solution of waveguide discontinuities by modal analysis," *IEEE Trans. Microw. Theor. Techn.*, vol. MTT-15, 1967, pp. 508–517.

18. Ahmed, S., "Finite element method for waveguide problems," *Elec. Lett.*, vol. 4, no. 18, 1968, pp. 387–389.

19. Silvester, P., "A general high-order finite element waveguide analysis program," *IEEE Trans. Microw. Theor. Techn.*, vol. MTT-17, 1969, pp. 204–210.

20. Silvester, P., "Finite element analysis of planar microwave networks," *IEEE Trans. Microw. Theor. Techn.*, vol. MTT-21, 1973, pp. 104–108.

21. Konrad, A., *Triangular finite elements for vector fields in electromagnetics*, Ph.D. Thesis, McGill University, 1974.

22. Konrad, A., "Vector variational formulation of electromagnetic fields in anisotropic media," *IEEE Trans. Microw. Theor. Techn.*, vol. MTT-24, 1976, pp. 553–559.

23. Ferrari, R.L., and Maile, G.L., "Three-dimensional finite method for solving electromagnetic problems," *Elec. Lett.*, vol. 14, no. 15, 1978, pp. 467–468.

24. Webb, J.P., Maile, G.L., and Ferrari, R.L., "Finite element solution of three-dimensional electromagnetic problems," *IEE Proc.*, vol. 130(H), no. 2, 1983.

25. Koshiba, M., Satoa, M., and Suzuki, M., "Application of the finite element method to E-plane waveguide discontinuities," *Trans. IECE Japan*, vol. E66, no. 7, 1983, pp. 457–458.

26. Webb, J.P., *Developments in finite element method three-dimensional electromagnetics problems*, Ph.D. Thesis, Cambridge University, 1981.

27. Silvester, P., and Ferrari, R.L., *Finite elements for electrical engineers*, Cambridge University Press, Cambridge.

28. Synge, J.L., *The hypercircle in mathematical physics*, Cambridge Press, Cambridge, Eng., 1957.

29. Webb, J.P., "Imposing linear constraints in finite element analysis," *to be submitted as a Short Communication in Int. J. Num. Met. Engng.*, 1988.

30. Kershaw, D.S., "The incomplete Cholesky-conjugate gradient method for the iterative solution of systems of linear equations," *J. Comp. Phys.*, vol. 26, 1978, pp. 43–65.

31. Helszajn, J., "Measurement of symmetrical waveguide discontinuities using the eigenvalue approach," *IEE Proc.*, vol. 127 , Part H, 1980, pp. 74–80.